Expression Ratios of the Anti-Apoptotic BCL2 Family Members Dictate the Selective Addiction of KSHV-Transformed Primary Effusion Lymphoma Cell Lines to MCL1

Daniel Dunham[a,b,c,] *, Prasanth Viswanathan[a,b,c,] *, Jackson Gill[d], Mark Manzano[a,b,c]#

[a]Department of Microbiology and Immunology, University of Arkansas for Medical Sciences, Little Rock, Arkansas, USA

[b]Center for Microbial Pathogenesis and Host Inflammatory Responses, University of Arkansas for Medical Sciences, Little Rock, Arkansas, USA

[c]Winthrop P. Rockefeller Cancer Institute, University of Arkansas for Medical Sciences Little Rock, Arkansas, USA

[d]Department of Biological Sciences, Henderson State University, Arkadelphia, Arkansas, USA

Running Head: MCL1 Addiction in KSHV-transformed PEL Cells

*D.D. and P.V. equally contributed to this article. Author order was determined based on project initiation.

#Address correspondence to Mark Manzano, mmanzano@uams.edu

Abstract Word Count: 247, Article Word Count: 4085

ABSTRACT

Kaposi's sarcoma-associated herpesvirus (KSHV) causes several malignancies in people living with HIV, including primary effusion lymphoma (PEL). PEL cell lines exhibit oncogene addictions to both viral and cellular genes. Using CRISPR screens, we previously identified cellular oncogene addictions in PEL cell lines, including MCL1. MCL1 is a member of the BCL2 family, which functions to prevent intrinsic apoptosis and has been implicated in several cancers. Despite the overlapping functions of the BCL2 family members, PEL cells are only dependent on MCL1 suggesting that MCL1 may have non-redundant functions. To investigate why PEL cells exhibit selective addiction to MCL1, we inactivated the intrinsic apoptosis pathway by engineering BAX/BAK1 double knockout cells. In this context, PEL cells become resistant to MCL1 knockdown or MCL1 inactivation by the MCL1 inhibitor S63845, indicating that the main function of MCL1 in PEL cells is to prevent BAX/BAK1-mediated apoptosis. The selective requirement to MCL1 is due to MCL1 being expressed in excess over the BCL2 family. Ectopic expression of several BCL2 family proteins, as well as the KSHV BCL2 homolog, significantly decreased basal caspase 3/7 activity and buffered against staurosporine-induced apoptosis. Finally, over-expressed BCL2 family members can functionally substitute for MCL1, when it is inhibited by S63845. Together our data indicate that the expression levels of the BCL2 family likely explain why PEL tumor cells are highly addicted to MCL1. Importantly, our results suggest that caution should be taken when considering MCL1i as a monotherapy regimen for PEL, because resistance can easily develop.

IMPORTANCE

Primary effusion lymphoma (PEL) is caused by Kaposi's sarcoma-associated herpesvirus. We previously showed that PEL cell lines require the anti-apoptotic protein MCL1 for survival, but

not the other BCL2 family proteins. This selective dependence to MCL1 is unexpected as the BCL2 family functions similarly in preventing intrinsic apoptosis. Recently, new roles for MCL1 not shared with the BCL2 family have emerged. Here, we show that non-canonical functions of MCL1 are unlikely essential. Instead, MCL1 mainly functions to prevent apoptosis. The specific requirement to MCL1 is due to MCL1 being expressed in excess over the BCL2 family. Consistent with this model, shifting these expression ratios changes the requirement away from MCL1 and towards the dominant BCL2 family gene. Together, our results indicate that although MCL1 is an attractive chemotherapeutic target to treat PEL, careful consideration must be taken as resistance to MCL1-specific inhibitors easily develops through BCL2 family overexpression.

KEYWORDS: KSHV, primary effusion lymphoma, MCL1, cell death, apoptosis, cell death, BCL2, vBCL2, S63845

56 **INTRODUCTION**

57 Kaposi's sarcoma-associated herpesvirus (KSHV) establishes lifelong latency in B cells. While
58 KSHV infections are often asymptomatic, they can develop into lymphoproliferative disorders
59 such as multicentric Castleman disease and primary effusion lymphoma (PEL) in people living
60 with HIV (1). PEL is a monoclonal B cell malignancy often found as effusions in body cavities
61 (2). Patients treated with modified etoposide, vincristine, and doxorubicin with
62 cyclophosphamide and prednisone (EPOCH) have a median survival time of 22 months and a
63 three-year survival rate of 47% (3). To date, no cancer-specific treatment is available for PEL.

64 PEL cell lines exhibit gene expression profiles closest to plasma cells (4-6) with elevated levels
65 of key plasma cell-associated transcripts such as the master transcription factor interferon
66 regulator factor 4 (IRF4) and genes involved in the unfolded protein response and endoplasmic
67 reticulum stress (ER) pathways (4, 7). The majority of PEL tumors (~80%) are also co-infected
68 with the related gammaherpesvirus Epstein-Barr virus (EBV). The presence of EBV appears to
69 improve prognosis in patients (3). Genetic analyses of PEL tumors do not show mutations or
70 translocations found in other hematological malignancies such as *TP53*, *MYC*, *BCL2*, or *BCL6*
71 (2, 8-10) although alterations in fragile site tumor suppressors have been reported (11). Instead,
72 the defining feature of PEL is that all tumor cells are latently infected with KSHV. The latent
73 virus constitutively expresses only a narrow subset of latency genes and at least 20 mature viral
74 microRNAs.

75 It is thought that constitutive expression of the KSHV latency genes drives the transformation of
76 PEL. Knockdown of the viral cyclin, viral FLICE inhibitory protein, viral interferon regulatory
77 factors 1-3 (vIRF1 to 3), or viral interleukin 6 all led to a decrease in survival of PEL cells in
78 culture (12-16). These latency genes regulate cellular networks to constitutively activate
79 pathways necessary to support the survival and proliferation of these infected cells. This creates

80 “oncogenic dependencies or addictions” to cellular genes, because tumor cells rely on the
81 continuous signaling of these pathways. For instance, addictions to several oncogenes have
82 been reported in PEL cell lines including the constitutive NF-κB signaling, phosphatidylinositol-
83 3-kinase-mTOR signaling, gp130-STAT3 signaling, high expression of the p53 inhibitor MDM2
84 and the IRF4 transcription factor, and c-Myc stabilization (9, 17-25).

85 We recently performed genome-wide CRISPR knockout screens to comprehensively identify
86 human oncogenic addictions or cellular genes that are required for the survival and/or
87 proliferation of PEL cell lines (26). Our study confirmed the addictions to well-described
88 pathways above. Importantly, we uncovered new dependencies that are consistently required in
89 eight different PEL cell lines which included genes that are commonly essential regardless of
90 cell type and genes that are strongly selective. Of note, we identify a strong addiction to the
91 myeloid cell leukemia-1 gene (MCL1). MCL1 belongs to the BCL2 gene family, of which there
92 are six members: MCL1, BCL2, BCL-xL (encoded by *BCL2L1*), BCL-W (encoded by *BCL2L2*),
93 A1 (encoded by *BCL2A1*), or Diva (encoded by *BCL2L10*). The BCL2 family functions to inhibit
94 intrinsic apoptosis. In healthy cells, monomers of the apoptotic effector BAX or BAK1 are
95 sequestered on the mitochondrial outer membrane (MOM) by the BCL2 family proteins (Fig.
96 1A). When intrinsic apoptosis is initiated, pro-apoptotic BH3-only proteins (e.g. PUMA, NOXA)
97 bind to the BCL2 family proteins to release the BAX/BAK1 monomers. The monomeric effectors
98 oligomerize to form pores in the MOM and trigger an apoptotic cascade (27). MOM
99 permeabilization is often considered to be the “point-of-no-return” for cell death.

100 Although the BCL2 family members share the same function in BAX/BAK1 sequestration, PEL
101 cell lines appear to be only addicted to MCL1 (Fig. 1B). In recent years, new roles beyond
102 apoptosis have been described for MCL1. MCL1 has been implicated in mitochondrial fusion,
103 respiration, fatty acid oxidation, and autophagy (28-30). In this study, we investigate the basis
104 for why KSHV-transformed PEL cell lines exhibit selective dependence on only MCL1 among

105 the BCL2 gene family. Here, we show that the main essential function of MCL1 in PEL cells is to
106 block intrinsic apoptosis and that non-canonical roles are unlikely. PEL cell lines likely depend
107 on MCL1 because it is expressed at 15-60-fold higher levels than the other BCL2 family
108 members. Altering the expression ratios by over-expression of the other BCL2-related proteins,
109 including the KSHV BCL2 homolog, rescues cells from intrinsic apoptosis induced by an
110 inhibitor of MCL1. This suggests that endogenous expression levels of the BCL2 proteins
111 determine the selective addiction to MCL1 in KSHV-transformed PEL cell lines.

112 **RESULTS**

113 **Primary effusion lymphoma cells are selectively addicted to MCL1**

114 We previously identified host gene addictions of KSHV-transformed PEL cell lines using
115 genome-wide CRISPR screens (26). Our work showed that these tumor cells require high
116 expression of the oncogene MCL1 for survival. Although the BCL2 family proteins share similar
117 roles in preventing intrinsic apoptosis (Fig. 1A), none of the other BCL2 family genes scored in
118 our CRISPR screens (Fig. 1B). To exclude the possibility that the selective addiction to MCL1 is
119 due to the absence of the other BCL2 family proteins, we performed Western blotting for
120 endogenously expressed BCL2, BCL-xL, BCL-W, A1, Diva, or MCL1 proteins in a panel of PEL
121 cell lines (Fig. 1C). This panel included five cell lines that are co-infected with EBV (BC-1, BC-2,
122 BC-5, CRO-AP5, and JSC-1) and five that are only infected with KSHV (APK-1, BC-3, BCBL-1,
123 BCLM, VG-1). Our immunoblots show that PEL cell lines uniformly express BCL-xL, BCL-W,
124 and MCL1. In contrast, BCL2 expression is detectable only in BC-1 and BC-3 cells, while we do
125 not detect A1 or Diva in any of the cell lines. Similar expression patterns of MCL1, BCL2, and
126 BCL-xL were recently reported in additional PEL cell lines (31).

127 To confirm the selective dependence of PEL cell lines to MCL1, we treated BC-1 or BC-3 cells
128 with small molecule inhibitors that are specific for MCL1 (S63845, “MCL1i”), BCL2 (ABT-
129 199/venetoclax, “BCL2i”) or BCL-xL (WEHI-539, “BCL-xLi”). These are not expected to cross-
130 inhibit the other BCL2 members. No BCL-W-specific inhibitors have been developed to date.
131 Consistent with our previous work (26), BC-1 and BC-3 cells are sensitive to MCL1i with an
132 estimated half maximal inhibitory concentration (IC50) of 177-228 nM (Fig. 1D). In contrast, both
133 cell lines are resistant to BCL2i and BCL-xLi. These results are consistent with a study showing
134 that PEL cell lines are sensitive to another MCL1i inhibitor AZD-5991 but are resistant to the
135 dual BCL2/BCL-xL inhibitor ABT-263 (31).

136 To further demonstrate that PEL cell lines selectively depend on MCL1 but not the other BCL2
137 family members, we targeted the endogenously expressed MCL1, BCL2, or BCL-xL for pooled
138 CRISPR knockout (KO) in BC-3 Cas9 cell lines. Our efforts to target BCL-W for CRISPR KO
139 were unsuccessful. Similar to what we previously observed (26), pooled MCL1 KO cells
140 significantly decreased cell viability by 70-90% as early as two days after transduction of
141 lentivirus encoding MCL1 guide RNAs (gRNAs) (Figs. 1E, 1F). In contrast, pooled BCL2, BCL-
142 xL, and BCL-W cells had similar viability compared to a negative control which targets the
143 *AAVS1* safe harbor locus (gAAVS1) for two weeks. In sum, our data indicate that PEL cell lines
144 express the other BCL2 family proteins, but are selectively addicted to MCL1.

145 **BAX/BAK1 double knockout cell lines**

146 Roles beyond inhibiting apoptosis have emerged for MCL1, including facilitating mitochondrial
147 respiration and fatty acid oxidation (28-30). We thus explored whether MCL1 may have critical
148 non-canonical functions in PEL cells that necessitate MCL1 expression, but not the expression
149 of other BCL2 proteins, in addition to its canonical role in inhibiting intrinsic apoptosis.

150 Loss-of-function studies on the non-canonical roles of MCL1 pose a technical hurdle because
151 these are confounded by effects from cell death. To address this issue, we derived clonal BAX
152 and BAK1 double knockout (DKO) cell lines from BC-1 (KSHV+EBV+) and BC-3 (KSHV+) cells
153 (Figs. 2A, 2B). This inactivates the intrinsic apoptosis pathway since pore formation by BAX or
154 BAK1 is considered the necessary step to irreversibly initiate intrinsic apoptosis (Fig. 1A).

155 We tested whether the DKO mutations successfully inactivate the intrinsic apoptotic pathway
156 after treatment with staurosporine. Staurosporine induces intrinsic apoptosis by broadly
157 inhibiting protein kinases. In parallel, we also tested the sensitivities of the DKO cells to different
158 antibiotics. Dose response curves for these inhibitors show that DKO cell clones are
159 substantially resistant to treatment with staurosporine, but remain sensitive to the antibiotics

160 puromycin, blasticidin, zeocin, and hygromycin (Figs. 2C-G). Our data thus confirm that our
161 DKO cell clones successfully inactivate the intrinsic apoptotic pathway but not other cell death
162 mechanisms.

163 **Knockout of BAX and BAK1 eliminates the dependency of PEL cells to MCL1**

164 We used the BC-1 and BC-3 DKO cell clones to investigate their dependency on MCL1. If
165 inactivation of MCL1 continues to affect the viability of DKO cells, this would suggest that MCL1
166 has an essential role in PEL that is independent of intrinsic apoptosis. In contrast, if the DKO
167 cells are unaffected by MCL1 inhibition, then the main essential function of MCL1 is to inhibit
168 BAX/BAK1-mediated cell death.

169 We therefore treated BC-1 and BC-3 wild type (WT) and DKO cells with increasing doses of the
170 MCL1 inhibitor S63845 (MCL1i) (32). Consistent with our previous work (26) and Fig. 1D, WT
171 BC-1 and BC-3 cells are sensitive to MCL1i (Fig. 3A). However, both DKO cell clones were
172 resistant to MCL1i and viable even at the maximum dose used (20 μM).

173 To confirm whether MCL1i induces apoptosis in PEL cells, we treated the WT and DKO cells
174 with a sublethal dose of MCL1i (100 nM) overnight and measured apoptotic markers using
175 Annexin V/7-AAD staining and Caspase 3/7 Luciferase Assay. We also included a sublethal
176 dose of staurosporine (20 nM) treatment as a positive control. Exposure to MCL1i or
177 staurosporine of BC-1 or BC-3 WT cells decreased live cells between 5-40% compared to the
178 DMSO control (Fig. 3B). This is accompanied by a proportional increase in cells undergoing
179 early and late apoptosis (Fig. 3B) as well as an increase in caspase 3/7 activities (Fig. 3C). In
180 contrast, all of these markers of programmed cell death are completely rescued in BC-1 and
181 BC-3 DKO cells. Thus, apoptotic cell death induced by the pharmacological inhibition of MCL1
182 is prevented by genetically ablating BAX and BAK1.

183 Since MCL1i was specifically designed to bind to the BH3-binding groove of MCL1 (32), it is
184 possible that MCL1i induces cell death by only inhibiting the anti-apoptotic role of MCL1 without
185 affecting putative non-canonical functions. We therefore targeted MCL1 for RNAi knockdown in
186 both BC-3 WT and DKO cells using a doxycycline (DOX)-inducible lentiviral shRNA. Total MCL1
187 protein was reduced by ~70% by quantitative Western blot in both WT and DKO cells using the
188 sh2MCL1 construct after Dox addition (Fig. 4A). This is not seen in the absence of DOX nor in a
189 negative control shRNA construct targeting the *Renilla* luciferase (33). Similar to our previous
190 work (26), MCL1 knockdown lead to a significant decrease in the total number of live cells in
191 BC-3 WT cells as early as two days after DOX treatment (Fig. 4B, dotted red line). This is
192 accompanied by a ~7-fold increase in caspase 3/7 activity (Fig. 4C). In contrast, MCL1
193 knockdown in BC-3 DKO cells did not substantially affect viability even after 12 days of DOX
194 treatment (Fig. 4B, dotted purple line) nor induce caspase 3/7 activity (Fig. 4C). We note the
195 efficiency of MCL1 knockdown is sustained at this time point as evidenced by reduced MCL1
196 protein (Fig. 4A, bottom). Taken together, our results from MCL1i treatment or shRNA
197 knockdown of the DKO cells suggest that the essential function of MCL1 in PEL cell lines is to
198 prevent intrinsic apoptosis.

199 **Over-expression of BCL2 proteins in PEL cell lines**

200 Our results thus far indicate that the main role of MCL1 in PEL cell lines is to inhibit cell death.
201 However, this does not address why we observe a selective addiction to MCL1 in our CRISPR
202 screens despite co-expression of functionally similar BCL2 proteins. Because a minimum
203 number of pro-survival BCL2 family protein molecules is required to successfully neutralize
204 BAX/BAK1 monomers and prevent pore formation, we hypothesized that the expression ratios
205 of the BCL2 family directly influence the addiction to MCL1. Although we detected BCL-xL and
206 BCL-W proteins in all PEL cell lines and BCL2 in BC-1 and BC-3 (Fig. 1C), Western blotting
207 does not allow for relative quantification between different proteins even in the same sample.

208 We therefore reanalyzed publicly available mRNA-seq datasets from different PEL cell lines
209 including other B cell malignancies to determine the abundance of the BCL2 family transcripts
210 (34). As seen in Figure 5A, endogenous MCL1 is the most highly expressed BCL2 family gene
211 in all six PEL cell lines. In contrast, BCL2, BCL-xL, and BCL-W mRNA levels are only modestly
212 expressed (15- to 60-fold less compared to MCL1) while A1 and Diva mRNAs are not detected.
213 This expression profile reflects the degree of depletion of gRNAs from the CRISPR screens
214 (Fig. 1B) consistent with the model that expression ratios of the BCL2 family may influence the
215 selective addiction to MCL1. Notably, these ratios and magnitude of MCL1 expression in PEL
216 cell lines are similar to what is seen in multiple myeloma cell lines which are also considered to
217 be plasma cell-like. This is consistent with previous reports demonstrating that the PEL and
218 multiple myeloma cell lines have similar gene expression profiles (4-6). These expression
219 patterns of the BCL2 family genes are distinct from those observed in other B cell malignancies
220 that represent different stages of B cell maturation (Fig. 5A). It is possible that the stoichiometry
221 of the BCL2 family members is a function of the stage of B cell differentiation.

222 If the skewed expression of MCL1 explains the dependency of PEL cell lines to this BCL2 family
223 member, we expect that changing the ratios of the BCL2 family genes would shift the
224 dependency to the most abundant BCL2 family protein and away from MCL1. We thus
225 transduced BC-1 or BC-3 cells with lentiviruses constitutively expressing the different BCL2
226 genes under the major immediate-early promoter and enhancer of the human cytomegalovirus
227 at a multiplicity of infection of 5. We chose to only over-express the proteins that are expressed
228 endogenously at the RNA and protein levels: BCL2, BCL-xL, BCL-W, or MCL1. In addition, we
229 also expressed the KSHV homolog of BCL2, vBCL2 (35, 36), that has been dually tagged with
230 FLAG-hemagglutinin (HA) epitopes at the N-terminus (N-vBCL2). Although vBCL2 is a lytic
231 gene and is not expressed in latently infected PEL cells, we were curious if this can functionally

232 substitute for MCL1 in PEL. Western blots confirm that each protein is expressed above
233 endogenous levels in both BC-1 and BC-3 backgrounds (Fig. 5B).

234 To confirm that the over-expressed proteins are functional in inhibiting intrinsic apoptosis, we
235 induced cell death in these cell lines using staurosporine and measured cellular viability using
236 CellTiterGlo 2.0 and apoptosis using Caspase 3/7 Luciferase Assay. All of the ectopically
237 expressed BCL2 family proteins and vBCL2 reduced basal caspase 3/7 activity in the absence
238 of staurosporine in both BC-1 and BC-3 cells (Figs. 5C, 5D). Reduction of caspase 3/7 activity
239 was consistently stronger in the BC-1 cell lines compared to the BC-3 cell lines. In both cases,
240 over-expression of BCL2, BCL-xL, or BCL-W inhibited basal caspase 3/7 activity the most while
241 MCL1 or N-vBCL2 had modest to no effects. It is possible that this minor effect of MCL1 or N-
242 vBCL2 in decreasing basal caspase 3/7 activity may be due to insufficient over-expression of
243 these proteins.

244 In the presence of staurosporine, naïve and mCherry-expressing cells had significantly reduced
245 cellular viability after overnight treatment as expected (Figs. 5E, 5F). Cell death was rescued in
246 all instances by all the BCL2 family proteins including N-vBCL2 although to a lesser extent
247 compared to the mCherry control. These effects in cell viability are conversely accompanied by
248 a reduction in caspase 3/7 activities (Figs. 5G, 5H). These experiments demonstrate that the
249 ectopically expressed BCL2 family proteins in BC-1 or BC-3 cells are functional in inhibiting
250 intrinsic apoptosis.

251 **Over-expression of BCL2 family proteins desensitizes PEL cells to MCL1i-induced**
252 **apoptosis**

253 We next tested whether over-expression of the BCL2-related proteins in BC-1 or BC-3 can shift
254 the dependency to a different BCL2 family protein and cause to cells to be less reliant to MCL1
255 for survival. We therefore inactivated MCL1 with MCL1i. Similar to staurosporine, overnight

256 treatment with MCL1i reduced the viability of naïve or mCherry-expressing cells (Fig. 6A). In
257 contrast, ectopic BCL2, BCL-xL, or BCL-W fully protected BC-1 and BC-3 cells against MCL1i
258 toxicity. N-vBCL2- and surprisingly, MCL1-expressing cells were sensitive to MCL1i with only a
259 marginal rescue of cell viability (20-30%) compared to mCherry. These effects in cell viability
260 are likely due to apoptosis as seen with the opposite pattern of caspase 3/7 activity in these cell
261 lines (Fig. 6B). Relative to naïve and mCherry-expressing cells, ectopic BCL2, BCL-xL, or BCL-
262 W inhibited caspase 3/7 activity induced by MCL1i to the same degree in both BC-1 and BC-3.
263 Ectopic N-vBCL2 moderately reduced caspase 3/7 activity while MCL1 had no measurable
264 effect.

265 Finally, we treated the cells with varying doses of MCL1i to calculate their relative sensitivities to
266 this inhibitor. Consistent with what we observed in Figs. 6A and 6B, over-expression of BCL2,
267 BCL-xL or BCL-W desensitized cells from MCL1i and increased the IC50 values by 100- to
268 1000-fold (Fig. 6C). The N-vBCL2 construct did not alter the over-all sensitivities of BC-1 or BC-
269 3 cells to MCL1i. While ectopic MCL1 increased the average MCL1i IC50 by ~2- (BC-3) to 3-fold
270 (BC-1), these effects were not statistically significant. In sum, our data demonstrates that
271 expression levels of the BCL2 family genes is the major determinant for the dependency to
272 MCL1 by PEL cell lines.

273

274

275 **DISCUSSION**

276 In this report, we explore why KSHV-transformed PEL cell lines exhibit selective addiction to the
277 oncogene MCL1, despite having shared functions with the related BCL2 family proteins. While
278 new roles beyond those shared with the other BCL2 family members have been attributed to
279 MCL1, we show that the essential function of MCL1 in PEL cell lines is to prevent intrinsic
280 apoptosis. This selective addiction to MCL1 is explained by the 15- to 60-fold stoichiometric
281 excess of MCL1 expression relative to other BCL2-related proteins as demonstrated by mRNA-
282 seq and functional rescue from MCL1i-induced cell death by over-expression of any of the BCL2
283 family proteins.

284 The failure to rescue MCL1i-induced apoptosis by the MCL1 or N-vBCL2 constructs may be due
285 to the degree of ectopic expression achieved in these cells. It is possible that the total amount of
286 BCL2 family proteins in any of these cases did not reach the minimum required to neutralize all
287 available MCL1i molecules.

288 It is not clear why BCL2 family expression is skewed towards MCL1 in PEL cell lines. We
289 speculate that this may be a consequence of the plasma cell-like B cell differentiation stage of
290 PEL tumors (4-6). Similarly, Fig. 5A and the Cancer Dependency Map (37) shows that multiple
291 myeloma cell lines, which are considered to be of plasma cell lineage, have high MCL1
292 expression and are selectively dependent on MCL1. In contrast, cell lines derived from B cell
293 malignancies representing earlier B cell stages have distinct expression patterns where the
294 other BCL2 family members are expressed at higher levels (Fig. 5A). Studies done in mice by
295 the Tarlinton group indicate that the requirements for the Bcl2 family members during B cell
296 development are dynamic and complex. It was shown that Mcl1 but not Bcl-xL is required for the
297 formation but not persistence of germinal center B cells and memory B cells using conditional
298 knockout models (38). This points to a transient dependence of antigen-specific B cells on Mcl1

299 for competition within germinal centers during maturation but not for their survival after their
300 establishment. Mcl1, however, is indispensable for the survival of plasma cells in culture and in
301 vivo in a tamoxifen-inducible Mcl1 knockout mouse model in a cell intrinsic manner (39). In
302 contrast, inducible knockout of Bcl-xL or treatment with ABT-737, a preferential inhibitor of BCL2
303 with modest effects on Bcl-xL and Bcl-W, have no effect in the survival of existing plasma cells
304 in culture or in vivo, respectively (39, 40). They propose that plasma cells require high levels of
305 Mcl1 along with other factors to provide an intrinsic survival potential in combination with
306 extrinsic survival signals from tissue-specific niches (e.g. secondary lymphoid tissues or bone
307 marrow) to ensure long-lived plasma cells (41). The requirement for the high expression of
308 MCL1 in plasma cells may be driven by master transcription factors such as IRF4 that occupy
309 lineage-specific super-enhancer regulatory regions. Indeed, we and others have identified a
310 super-enhancer element around the MCL1 locus bound by IRF4 in PEL cell lines (21, 42, 43).

311 Upon activation and during maturation, B cells undergo dramatic changes to support their
312 effector functions in immune defense (Reviewed in 44). A large part of the plasma cell
313 differentiation program is the remodeling and expansion of the endoplasmic reticulum (ER) to
314 prepare for immunoglobulin production and secretion (45). Nutrient transporters and metabolic
315 enzymes are upregulated to sustain antibody production and organelle maintenance by the
316 lineage transcription factor Blimp-1 (46). High expression of MCL1 may thus act as a buffer
317 from this increased ER stress and metabolic load to ensure the survival of these B cells.
318 Knockdown of the glucose transporter GLUT4 in multiple myeloma cell lines induced apoptosis
319 by decreasing MCL1 mRNA expression (47), thereby supporting this link between metabolism
320 and apoptosis.

321 In the case of PEL, the infected tumor cells neither express nor secrete immunoglobulin
322 molecules. However, recent work from the Gottwein laboratory shows that PEL cell lines need
323 to constitutively counteract death signals originating from the ER and Golgi compartments in the

324 absence of any exogenous trigger (48). Consistent with this, PEL cell lines have elevated
325 expression of genes involved in the unfolded protein response, often triggered by ER stress (4).
326 These suggest that the ER and Golgi bodies in PEL cells are also under stress despite the
327 absence of antibody production. In line with this, KSHV is known to activate ER stress
328 responses during lytic reactivation (49, 50). Therefore, KSHV needs to counter these ER, Golgi
329 and metabolic stresses by possibly reinforcing or amplifying existing survival pathways in
330 plasma cells such as MCL1. More recently, the latency-associated nuclear antigen (LANA) was
331 shown to indirectly enhance the steady state levels of the MCL1 protein by binding to the E3
332 ubiquitin ligase FBW7 and preventing MCL1 degradation (51). As mentioned above, although
333 we find binding sites for the lineage transcription factor IRF4 on the MCL1 super-enhancer in
334 PEL cells, we recently reported that the B cell-specific latency gene vIRF3 largely co-occupies
335 similar sites as IRF4, including the MCL1 super-enhancer and promoter (21). This suggests that
336 vIRF3 may function to enhance MCL1 expression. We are currently investigating how vIRF3
337 regulates MCL1 expression at the transcriptional level.

338 A parallel relationship between lineage-specific expression and dependence to the BCL2 family
339 proteins is also seen in lymphatic endothelial cells (LECs) which are thought to be candidates
340 for the cellular origin of Kaposi's sarcoma spindle cells (52). In this case, LECs express and
341 depend on high levels of BCL-xL instead of MCL1 for survival. This dependency dramatically
342 increases during KSHV infection (Dr. Michael Lagunoff, personal communication) which
343 supports the model where the virus reinforces pro-survival pathways already present in the cell.

344 The selective dependence of PEL cell lines to MCL1 makes it an attractive target for therapy.
345 We have previously shown that the MCL1 protein is highly expressed in primary tumors from
346 patients (26). Candidate MCL1-selective drugs are now in various stages of clinical trials to treat
347 hematologic malignancies (53) and have the potential to be repurposed to treat PEL.
348 Venetoclax, the first approved BH3 mimetic drug, has over-all response rates of ~80% in

349 relapsed and/or refractory chronic lymphocytic leukemia (54) and ~75% in relapsed and/or
350 refractory mantle cell lymphoma (55) with a durable response even after ~3 years (56).
351 However, other cancers like acute myelogenous leukemia exhibit a lower response rate to
352 venetoclax (19%) where non-responsive patients had an increase in BCL-xL or MCL1
353 expression (57). Our data similarly shows that over-expression of any of the BCL2 family
354 proteins or loss of BAX or BAK1 leads to resistance to MCL1 inhibitors. Thus, care must be
355 taken when testing MCL1 inhibitors in PEL patients to avoid resistance. One strategy is using
356 high but tolerable doses of MCL1 drugs to minimize selection for resistant tumor cells. Another
357 approach is to combine this with other regimens that do not act on the same pathway. These
358 strategies need to be explored to provide the most effective treatment for KSHV-induced PEL.

359 **MATERIALS AND METHODS**

360 **Cells**. Cells were cultured as described (21). HEK293T cells were cultured in Dulbecco's
361 modified Eagle medium with L-glutamine and 4.5 g/L glucose (Corning Life Sciences,
362 Tewksbury, MA) supplemented with 10% Serum Plus II medium (Millipore-Sigma, Burlington,
363 MA) and 10 µg/ml gentamicin (Gibco, Waltham, MA). BC-1 and BC-3 cell lines were grown in
364 RPMI 1640 (Corning) supplemented with 10 µg/ml gentamicin (Life Technologies, Carlsbad,
365 CA), 0.05 mM β-mercaptoethanol (Sigma-Aldrich, St. Louis, MO), and 10% (BC-1) or 20% (BC-
366 3) Serum Plus II medium. All PEL cell lines were grown at 37°C with 5% CO_2 and maintained at
367 log phase between $2x10^5$ and $1x10^6$ cells/mL.

368 **Primers and synthetic genes.** All primers were purchased from Integrated DNA Technologies
369 (Coralville, IO). Synthetic genes for eGFP fragment, shRNA cassettes and MCL1 cDNA were
370 synthesized by Twist Bioscience (South San Francisco, CA). Sequences and primer
371 combinations for cloning are listed in Tables 1 and 2.

372 **shRNAs.** A self-inactivating version of the pLVX-TetOne-Zeo lentiviral vector (58) (a gift from
373 Dr. Britt Glaunsinger) was first made via PCR mutagenesis. A deletion in the U3 region of the
374 3'LTR was introduced using primer pairs 169/171 and 172/170. The PCR products were fused
375 with primers 169/170 and cloned into pLVX-TetOne-Zeo using the KpnI and NheI restriction
376 sites (New England Biolabs, Ipswich, MA). The new vector is renamed pLVX-SIN-TetOne-Zeo
377 (pSTZ) to denote the self-inactivating deletion (SIN).

378 shRNAs were designed using the SplashRNA algorithm (33) using default parameters
379 (http://splashrna.mskcc.org). sh2MCL1 was synthesized as a gene fragment (Twist Bioscience)
380 while shREN was amplified from pZIP-ZsGreen-T2A-Hyg-shRen.713 (48). These shRNA
381 cassettes were assembled in the 3'UTR of a synthetic eGFP gene (Twist Bioscience) via two-
382 fragment Gibson assembly into the pSTZ backbone linearized by EcoRI and BamHI (NEB).

383 **BCL2 cDNAs**. cDNAs for human BCL2, BCL-xL, and BCL-W were amplified from pCDNA3-HA-
384 BCL2, pCDNA-HA-BCL-xL (59) (gifts from Dr. Timothy Chambers), and pLX304-BCL2L2 (Clone
385 # HsCD00440394 from Human ORFeome Collection from DNASU (60)). vBCL2 sequence was
386 amplified from BC-1 genomic DNA. The Flag-HA dual tag cassette was amplified from pLC-
387 FLAG-HA-vIRF3-P2A-hyg (Manzano and Gottwein, unpublished). Internal restriction sites were
388 repaired using PCR mutagenesis. Details on primer sequences and primer combinations for
389 each PCR step are listed in Tables 1 and 2.

390 **Lentiviruses**. The day prior to transfections, 4-5x10^6 293T cells were plated in 10 cm dishes.
391 Lentiviral transfer vectors (5 μg) were co-transfected with pMD2.G (2.44 μg) and psPAX2 (3.74
392 μg) packaging vectors and 39.13 μL 1 mg/mL polyethylenimine (Sigma Catalog #408727) in
393 500 μL OptiMEM (Gibco). After 4-6 hours, media was replaced with complete RPMI medium
394 supplemented with 10% Serum Plus II medium. Supernatants containing lentiviruses were
395 harvested after three days by filtering through a 0.45 μm pore membrane.

396 Lentiviral titers were determined by functional titration. Increasing volumes of supernatant
397 containing lentiviruses were added to 1x10^5 naïve BC-1 or BC-3 cells in 0.5 mL media with 0.5
398 μL 8 μg/mL polybrene. The day after, appropriate antibiotics were added to select for infected
399 cells. Number of surviving cells was compared to uninfected cells to determine infection rates
400 and viral titers. Final lentiviral transductions were performed in 4x10^5 BC-1 or BC-3 cells in 2 mL
401 media with 8 μg/mL polybrene at defined MOIs.

402 **Generation of BAX/BAK1 DKO cells**. Two gRNAs targeting the human *BAX* or *BAK1* gene
403 were chosen from the genome-wide Brunello CRISPR library to increase the efficiency of editing
404 in all alleles (61). Based on these gRNAs, primer pairs were designed to create dsDNA
405 duplexes with compatible BbsI overhangs. These primer pairs were assembled by heat-

406 denaturation and annealing in Buffer 3.1 (NEB), then cloned into BbsI-linearized pX458 (62) (a
407 gift from Dr. Feng Zhang, Addgene #48138).

408 BC-1 and BC-3 cells were adjusted to $2x10^5$ cells/mL the day before transfection. On the day of
409 transfection, $1x10^6$ BC-1 or BC-3 cells were pelleted in 50 mL tubes at 90g, for 10 min. Each
410 pellet was carefully resuspended in 20 μL of SF Cell Line Nucleofector Solution with
411 Supplement 1 (Lonza Cat. #V4XC-2032, Basel, Switzerland) and 1.5 μL of pX458 plasmids (150
412 ng each of BAX g2, BAX g3, BAK1 g1, BAK1 g3; 600 ng total). Cells transferred to
413 Nucleocuvette strips and pulsed with program CA-189 using the 4D-Nucleofector X (Lonza).
414 Transfection reactions were allowed to recover at room temperature for 10 min. Afterwards, 80
415 μL of pre-warmed complete media was added. Cells in the Nucleocuvette strips were incubated
416 at 37°C for 10 min. Finally, cells were collected with an additional 120 μL of pre-warmed
417 complete media and transferred to a round-bottom 96-well plate. Cells were expanded for 5-7
418 days to at least $2x10^6$ total cells. Two additional rounds of nucleofection were performed as
419 above to ensure efficient editing in all four alleles.

420 After a week of recovery from the third nucleofection, cells were individually cultured in round
421 bottom 96-well plate using dilution cloning. Clones were screened for successful editing. We
422 first triaged the clones based on the absence of full length BAX and BAK1 proteins by Western
423 blotting. Next, we further screened clones using genotyping primers (189 and 190 for *BAX*; 215
424 and 216 for *BAK1*). We would expect that simultaneous cutting of the two guides in an allele will
425 lead to ~100-400 bp deletions that can be distinguished from wt or single cut alleles by PCR.
426 While this assay does not discriminate between unedited from single editing events, this allows
427 us to limit our final validation to those with at least one allele deleted. Finally, we confirmed
428 frameshift indels by amplifying the targeted loci for Sanger or Illumina sequencing. Illumina

429 sequencing and analysis were performed by the Massachusetts General Hospital Center for
430 Computational and Integrative Biology DNA Core Facility.

431 **CRISPR targeting of BCL2 family**. Clonal BC-1 Cas9 or BC-3 Cas9 cells (26) were transduced
432 with lentiviruses encoding gRNAs targeting the BCL2 family genes at MOI 1. gRNAs targeting
433 BCL2 or BCL-W were cloned in pLentiGuide (Addgene #117986) that was linearized with BsmBI
434 (NEB). gRNAs for gAAVS1, BCL-xL and MCL1 have been previously cloned and described
435 (26). Live cells were measured every 2-3 days on the BD FACS Celesta Flow Cytometer (BD
436 Biosciences, Franklin Lakes, NJ) using a known amount of spike-in AccuCount Blank particles
437 (Spherotech, Lake Forest, IL, Cat. #ACBP-50-10). Data analysis was performed using FlowJo
438 v10.8.1 software (BD Biosciences). Cells were split to 3 x 10^5 cells/mL to ensure that all cells
439 were continuously dividing.

440 **Western blots.** Cells were washed with phosphate buffered saline and lysed with RIPA lysis
441 buffer (50 mM Tris, 150 mM NaCl, 1% IGEPAL CA-630, 0.5% sodium deoxycholate, 0.1%
442 sodium dodecyl sulfate, pH 7.4) with protease inhibitor cocktail III (Calbiochem, EMD Millipore).
443 Lysates were incubated on ice for 10 minutes and clarified by spinning at 12,000 g for 10
444 minutes. Total protein was quantified the Pierce BCA Protein Assay Kit (Thermo Fisher).

445 Equivalent amounts of total proteins were run in Bolt 4%-12% Bis-Tris gradient gels (Thermo
446 Fisher Scientific) or 15% tris-glycine-SDS acrylamide gels and transferred to 0.2 µm-pore size
447 nitrocellulose membranes in Towbin buffer (25 mM Tris, 192 mM glycine, 20% methanol, pH
448 8.3) for 90 min at 400 mA. Membranes were blocked with a 1:3 dilution of Intercept (TBS)
449 Blocking Buffer (Li-Cor Biosciences, Lincoln, NE) in TBS for 1 h at room temperature.
450 Membranes were incubated with primary antibodies diluted 1:3000 in blocking buffer–0.1%
451 Tween 20 overnight at 4°C. Primary antibodies were purchased from Cell Signaling Technology
452 (Danvers, MA): anti-BCL2 clone D55G8, anti-BCL-xL clone 54H6, anti-BCL-W clone 31H4, anti-

453 MCL1 clone D2W9E, anti-HA clone C29F4, anti-A1 clone D1A1C, anti-Diva (Catalog # 3869),
454 anti-BAK clone D4E4, and anti-BAX clone D2E11; or Sigma: anti-beta-actin clone AC-15 and
455 anti-alpha-tubulin clone B-5-1-2; or Santa Cruz Biotechnology (Dallas, TX): anti-GAPDH clone
456 0411.

457 Immunoblots were washed five times with TBST for 5 min each then incubated for 1 hour with
458 IRDye 800 CW-conjugated secondary antibodies (Li-Cor Biosciences) diluted in TBS (1:20,000).
459 Membranes were finally washed four times with TBST and once in TBS. Western blots were
460 imaged on the Odyssey Fc or M Imager (Li-Cor Biosciences).

461 **Dose Response Curves**. Serial dilutions of the different inhibitors/drugs were added to each
462 well containing 5 x 10^3 BC-1 or BC-3 cells in a U-bottom 96-well plate. At designated time points
463 (2 days for puromycin (Cayman Chemicals, Ann Arbor, MI); 3 days for MCL1i
464 (MedChemExpress, Monmouth Junction, NJ), ABT-199 (Tocris Bioscience, Minneapolis, MN),
465 WEHI-539 (APExBIO, Houston, TX) and staurosporine (APExBIO); 6 days for blasticidin
466 (Gibco), zeocin (Invivogen, San Diego, CA), and hygromycin (Gibco)), 20 µL aliquots of the cells
467 were used to measure cell viability using 20 µL CellTiter-Glo 2.0 Cell Viability Reagent
468 (Promega). Luminescence was read using Synergy H1 microplate reader (Biotek, Winooski, VT)
469 with an integration time of 2 sec. Raw luminescence readings were normalized as a percentage
470 of the DMSO control. Normalized values were used to calculate the IC50 using the "[inhibitor]
471 vs. normalized response (variable slope)" function in Prism 9 (GraphPad, San Diego, CA).

472 **Caspase 3/7 Assay**. 2 x 10^4 BC-1 or BC-3 cells were seeded in each well of a U-bottom 96-well
473 plate and treated with staurosporine (20 nM for BC-1, 100 nM for BC-3), 100 nM MCL1i, or
474 DMSO. These concentrations were chosen because they approximate the IC50 values of each
475 drug for each cell line. After 24 hours, 20 µL of cells were mixed with 20 µL of the CellTiter-Glo
476 2.0 Cell Viability Reagent or Caspase-Glo 3/7 Assay substrate (Promega). Luminescence was

477 measured after 2 min incubation for CellTiter-Glo 2.0 or 30 min incubation for Caspase-Glo 3/7
478 Assay using the Synergy H1 microplate reader as above. Raw luminescence values for caspase
479 3/7 activities were sequentially normalized to the matched raw CellTiter-Glo 2.0 readings, then
480 to the DMSO controls and finally, to the mCherry-expressing cell line.

481 **Annexin V/7-AAD staining**. BC-1 or BC-3 wt or DKO cells (4 x 10^5 cells/mL, 3 mL plated in 6-
482 well plate) were treated overnight with DMSO, 20 nM staurosporine, or 100 nM MCL1i. 7 x 10^5
483 live cells were pelleted and washed twice with wash buffer (2% bovine serum albumin in PBS).
484 Cells were resuspended in 100 µL Annexin V Binding Buffer (Biolegend, San Diego, CA). Cells
485 were stained for 15 min in the dark with 5 µL APC Annexin V (Biolegend) and 5 µL 7-AAD
486 Viability Staining Solution (Biolegend). After incubation, 400 µL of Annexin V Binding Buffer was
487 added and the cells were analyzed on a flow cytometer. In parallel, cellular viability and caspase
488 3/7 activities were measured as described above from 20 µL aliquots.

489

490 **ACKNOWLEDGMENTS**

491 We thank Logan Moorhead for initial help with engineering the DKO cell lines, Dr. Eva Gottwein
492 for the pZIP-ZsGreen-T2A-Hyg-shRen.713 and pLC-FLAG-HA-vIRF3-P2A-hyg plasmids, Dr.
493 Britt Glaunsinger for the pLVX-TetOneZeo plasmid, and Dr. Timothy Chambers for the BCL-xL
494 and BCL2 expression vectors. We thanks Drs. Eva Gottwein, Youssef Aachoui, Changhoon Oh,
495 and J. Craig Forrest for helpful discussion and feedback on the manuscript.

496 This work is supported by a Transition Career Development Award K22 CA241355 from the
497 National Cancer Institute of the National Institutes of Health (NIH) to M.M. Additional support
498 was provided by the Center for Microbial Pathogenesis and Host Inflammatory Responses
499 program grant P20 GM103625 from the National Institute of General Medical Sciences (NIGMS)
500 of the NIH, Winthrop P. Rockefeller Cancer Institute at UAMS, and an equipment grant from the
501 UAMS Office of the Vice Chancellor for Research and Innovation. J.G. is a recipient of the
502 Undergraduate Summer Research Fellowship from the Arkansas IDeA Network of Biomedical
503 Research Excellence (INBRE) funded by program grant P20 GM103429 from NIH/NIGMS. The
504 content is solely the responsibility of the authors and does not necessarily represent the official
505 views of the funding bodies. The authors declare no conflicts of interests.

506

507 **FIGURE LEGENDS**

508 **Figure 1. *A***. The BCL2 family proteins (including MCL1) block intrinsic apoptosis by
509 sequestering activated BAX or BAK1 monomers on the outer membrane of the mitochondria.
510 During intrinsic apoptosis, pro-apoptotic BH3-only proteins inactivate the BCL2 family proteins
511 and release the BAX/BAK1 monomers. Free monomers assemble to create mitochondrial pores
512 and release cytochrome c to initiate the apoptotic cascade in the cytoplasm. ***B***. Only gRNAs
513 targeting MCL1 among the BCL2 family are significantly depleted in all PEL cell lines that were
514 previously screened (26). ***C***. Western blots of the different BCL2 family proteins in a panel of
515 PEL cell lines that are infected with KSHV only or co-infected by KSHV and EBV. A1 and Diva
516 proteins are not detected. ***D.*** Dose-response curves of BC-1 and BC-3 cells treated with MCL1i,
517 BCL2i or BCL-xLi. ***E***. Cumulative live cell plot of BC-3 Cas9 cells that were transduced with
518 lentiviruses expressing gRNAs against AAVS1, MCL1, BCL2, or BCL-xL. MCL1 g1 and g2 cells
519 were not counted beyond day 2 because of low number of live cells. Statistical differences were
520 calculated using two-way ANOVA with Dunnett's multiple comparison test (n=3). ***F***.
521 Representative Western blots of MCL1, BCL2, BCL-xL, or GAPDH at day 2 from panel E.
522 Samples targeting MCL1 and BCL-xL were ran on the same gel flanking the same gAAVS1
523 control.

524 **Figure 2. *A.*** Summary of CRISPR edits in BC-1 BAX/BAK1 double knockout (DKO) clone #28
525 and BC-3 DKO clone #12. ***B.*** Western blots for BAX, BAK1 and tubulin proteins of WT or DKO
526 cells in panel A. . ***C-G.*** Dose response curves of BC-1 or BC-3 cells with BAX/BAK1 wildtype or
527 DKO background upon exposure to different inducers of cell death: *C*. staurosporine, *D.*
528 puromycin, *E*. blasticidin, *F.* hygromycin, or *G***.** zeocin. Statistical differences were calculated
529 using two-way ANOVA with Tukey's multiple comparison post-hoc test (n=3). Adjusted *p* values
530 reflect post-hoc comparisons between the responses of the wt cell line compared to the DKO
531 cell line at the specific time point. Error bars, standard error of mean. n.s., not significant.

532 **Figure 3.** ***A***. MCL1i dose response curves of BC-1 or BC-3 cells with BAX/BAK1 WT or DKO
533 background. ***B.*** Distribution of live, early apoptotic or late apoptotic cell populations of BC-1 and
534 BC-3 WT or DKO cells after an overnight treatment of 100 nM MCL1i or 20 nM staurosporine as
535 determined by Annexin V/7AAD staining. ***C***. In parallel, caspase 3/7 activities were measured
536 using a luciferase assay from cells in panel B. Statistical differences were calculated using one-
537 way ANOVA with Tukey's multiple comparison test (n=3). Error bars, standard error of mean.
538 n.s., not significant.

539 **Figure 4.** ***A***. Western blots for total MCL1 in BC-3 BAX/BAK wt or DKO #12 cells transduced
540 with lentiviruses expressing a doxycycline (DOX)-inducible shRNA against Renilla luciferase or
541 MCL1. Shown are samples taken after 2, 3, or 12 days of DOX-treatment (1 µg/mL). ***B.***
542 Cumulative live cell count of BC-3 cells upon DOX treatment (dotted lines). Cell counts were
543 terminated for DOX-treated BC-3 wt cells with sh2MCL1 (dotted red line) at day 9 of DOX-
544 treatment due to significant amount of cell death. Statistical differences were calculated using
545 one- or two-way ANOVA with Tukey's multiple comparison test (n=3). One-way ANOVA for
546 each time point was instead done for *C*. since two-way ANOVA requires matched data for all
547 time points. Adjusted *p* values reflect post-hoc comparisons between the responses of the wt
548 cell line compared to the DKO cell line at the specific time point or Dox-treated cell line
549 compared to matched untreated cell line (n=3). C. Caspase 3/7 activities were measured using
550 a luciferase assay from cells after 2 days of DOX treatment. Statistical differences were
551 calculated using one-way ANOVA with Tukey's multiple comparison test (n=3). Error bars,
552 standard error of mean. n.s., not significant.

553 **Figure 5.** ***A***. Normalized expression values (fragments per kilobase of exon per million mapped
554 fragments, FPKM) of BCL2 family transcripts in B cell lines representing different malignancies
555 and stage of B cell differentiation from the Cell Model Passports database (34). These cancers
556 include: pre-B cell acute lymphoblastic leukemia (pre-B-ALL), mantle cell lymphoma (mantle

557 CL), follicular lymphoma (FL), Burkitt lymphoma (EBV-infected or uninfected), diffuse large B
558 cell lymphoma germinal center subtype (DLBCL GC) or activated B cell subtype (DLBCL ABC),
559 chronic lymphocytic leukemia (CLL), multiple myeloma and PEL. ***B.*** Western blots of the BCL2
560 family members and HA-tagged vBCL2 in BC-1 or BC-3 cells transduced with lentiviruses over-
561 expressing these cDNAs. ***C-D.*** Basal caspase 3/7 activity of BC-1 (n=11) or BC-3 cells (n=7)
562 normalized to total live cells measured by a caspase 3/7 luciferase assay. ***E-F.*** Cell viability
563 measured by CellTiterGlo 2.0 assay or ***G-H.*** relative caspase 3/7 activity in live BC-1 (n=3) or
564 BC-3 cells (n=4) after overnight treatment of 20 nM or 100 nM staurosporine. Statistical
565 differences were calculated using one- or two-way ANOVA with Tukey's multiple comparison
566 post-hoc test. Adjusted *p* values reflect post-hoc comparisons between the cell lines in response
567 to staurosporine or DMSO unless indicated otherwise. Error bars, standard error of mean. n.s.,
568 not significant.

569 **Figure 6.** ***A.*** Cell viability measured by CellTiterGlo 2.0 assay or ***B.*** relative caspase 3/7 activity
570 in live BC-1 or BC-3 cells over-expressing BCL2 family cDNAs after overnight treatment of 100
571 nM MCL1i. Statistical differences were calculated using one- or two-way ANOVA with Tukey's
572 multiple comparison test (n=5). Adjusted *p* values reflect post-hoc comparisons between the cell
573 lines in response to staurosporine or DMSO unless indicated otherwise. ***C.*** IC50 values of
574 MCL1i in BC-1 or BC-3 cells. For BC-1, one-way ANOVA with Tukey's multiple comparison test
575 was used for statistical tests (n≥3). Since BC-3 cell lines over-expressing BCL2, BCL-xL or
576 BCL-W were highly resistant to MCL1i even at high doses, IC50 values derived from these
577 incomplete sigmoidal dose-response curves had low confidence intervals. Thus, non-parametric
578 Kruskal-Wallis post-test was used. Adjusted *p* values reflect post-hoc comparisons between the
579 cell lines to the mCherry control. Error bars, standard error of mean. n.s., not significant.

580

584 **TABLES**

585 **Table 1. Primer sequences.**

5	CACCGACGGCAGCTCGCCATCATCG
6	AAACCGATGATGGCGAGCTGCCGTC
50	GCTAGCGCTACCGGTGCCGCCACCATGGCGCACGCTGGGAGAACAGGG
51	GGGAGAGGGGCGGATCCTCACTTGTGGCCCAGATAGGC
54	GCTAGCGCTACCGGTGCCGCCACCATGTCTCAGAGCAACCGGGAGCTGG
55	GGGAGAGGGGCGGATCCTCATTTCCGACTGAAGAGTGAGCCC
56	CCACCTAGAGCCTTGGATTCAGGAGAACGGCGGCTGG
57	CCAGCCGCCGTTCTCCTGAATCCAAGGCTCTAGGTGG
62	GCTAGCGCTACCGGTGCCGCCACCATGGCGACCCCAGCCTCGGCCCCAG
63	GGGAGAGGGGCGGATCCTCACTTGCTAGCAAAAAAGGCCCCTAC
64	GCAGCTGGCTGACTGGATTCACAGCAGTGGGGGCTGG
65	CCAGCCCCCACTGCTGTGAATCCAGTCAGCCAGCTGC
66	CCCGATTACGCTAGCGGCGACGAGGACGTTTTGCCT
67	AGGCAAAACGTCCTCGTCGCCGCTAGCGTAATCGGG
68	GAGATTTCACAGCACCACTGGTATAAACCAGCTTGGG
69	CCCAAGCTGGTTTATACCAGTGGTGCTGTGAAATCTC
70	GGGAGAGGGGCGGATCCTTATCTCCTGCTCATCGCGACCGC
97	CACCGTTTCATCCAGGATCGAGCA
98	AAACTGCTCGATCCTGGATGAAAC
99	CACCGGACGAACTGGACAGTAACA
100	AAACTGTTACTGTCCAGTTCGTCC
103F	CACCGCTCACCTGCTAGGTTGCAG
103R	AAACCTGCAACCTAGCAGGTGAGC
161	GACACCGGTGCAGCGGCCGCTGTTTGAATGAGGCTTCAGTAC
162	GTCCAGCTTAGCTCGCAGGGGAGGTGGTCTGGATCCTAAAGTGATTTAAT TTATACCATT
169	CTACCAATGCTGATTGTGCCTGGC
170	AACAGCTATGACCATGATTACGCC
171	CTAACCAGAGAGACCCAGTACAGTCCGGATGCAGCTCTCGGGCCAC
172	GTGGCCCGAGAGCTGCATCCGGACTGTACTGGGTCTCTCTGGTTAG
189	GAGTTTGAGGTCTGATTATTGTGG
190	GAAGTTGCCGTCAGAAAACATGTC
197	CACCGGCCTTCTTTGAGTTCGGTG
198	AAACCACCGAACTCAAAGAAGGCC
199	CACCGCTGACGCCCTTCACCGCGCG
200	AAACCGCGCGGTGAAGGGCGTCAGC
215	CTCCCTGACTCCCAGCTTTG
216	CCTGGTGGCAATCTTGGTGA
219	CACCGAGACAAAGAAGGCTACAAGG
220	AAACCCTTGTAGCCTTCTTTGTCTC
221	CACCGTGTGCTGAGAGTGTCAACA
222	AAACTGTTGACACTCTCAGCACAC
EHG4087	GAGCTGGTTTAGTGAACCG
eGFP cassette	ACTTTCCGTACCACTTCCTACCCTCGTAAAGAATTCATGGTGAGCAAGGGC GAGGAGCTGTTCACCGGGGTGGTGCCCATCCTGGTCGAGCTGGACGGCG

	ACGTAAACGGCCACAAGTTCAGCGTGTCCGGCGAGGGCGAGGGCGATGC CACCTACGGCAAGCTGACCCTGAAGTTCATCTGCACCACCGGCAAGCTGC CCGTGCCCTGGCCCACCCTCGTGACCACCCTGACCTACGGCGTGCAGTG CTTCAGCCGCTACCCCGACCACATGAAGCAGCACGACTTCTTCAAGTCCG CCATGCCCGAAGGCTACGTCCAGGAGCGCACCATCTTCTTCAAGGACGAC GGCAACTACAAGACCCGCGCCGAGGTGAAGTTCGAGGGCGACACCCTGG TGAACCGCATCGAGCTGAAGGGCATCGACTTCAAGGAGGACGGCAACATC CTGGGGCACAAGCTGGAGTACAACTACAACAGCCACAACGTCTATATCAT GGCCGACAAGCAGAAGAACGGCATCAAGGTGAACTTCAAGATCCGCCACA ACATCGAGGACGGCAGCGTGCAGCTCGCCGACCACTACCAGCAGAACAC CCCCATCGGCGACGGCCCCGTGCTGCTGCCCGACAACCACTACCTGAGC ACCCAGTCCGCCCTGAGCAAAGACCCCAACGAGAAGCGCGATCACATGGT CCTGCTGGAGTTCGTGACCGCCGCCGGGATCACTCTCGGCATGGACGAG CTGTACAAGTAGGACACCGGTG CAGCGGCCGCTGTTTGAATGAGGCTTCAGTACTTTACAGA
sh2MCL1 cassette	TGTTTGAATGAGGCTTCAGTACTTTACAGAATCGTTGCCTGCACATCTTGG AAACACTTGCTGGGATTACTTCTTCAGGTTAACCCAACAGAAGGCTAAAGA AGGTATATTGCTGTTGACAGTGAGCGCTCCCAGTATACTTCTTAGAAATAG TGAAGCCACAGATGTATTTCTAAGAAGTATACTGGGAATGCCTACTGCCTC GGACTTCAAGGGGCTACTTTAGGAGCAATTATCTTGTTTACTAAAACTGAAT ACCTTGCTATCTCTTTGATACATTTTTACAAAGCTGAATTAAAATGGTATAAA TTAAATCACTTTAGGATCCAGACCACCTCCCCTGCGAGCTAAGCTGGAC

586

587

588 **Table 2. Combinations of primers used for cloning constructs.**

Construct	PCR	Primers	Template	Source
pLV-SIN-TetOne-ZeoR (pSTZ)	1	169, 171	pLVX-TetOne-Zeo	(58)
	2	170, 172		
	Overlap	169, 170	PCR 1 and 2	
shREN	N/A	161, 162,	pZIP-ZsGreen-T2A-Hyg-shRen.713	(48)
BCL2	N/A	50, 51	pCDNA3 HA-BCL2	(59)
BCL-xL	1	54, 57	pcDNA3 HA-BCL-xL	
	2	55, 56		
	Overlap	54, 55	PCR 1 and 2	
BCL-W	1	62, 65	pLX304 BCL2L2	DNASU
	2	63, 64		
	Overlap	62, 63	PCR 1 and 2	
vBCL2 N-FLAG-HA	1	EHG4087, 67	pLC-FLAG-HA-vIRF3-P2A-hyg	Manzano & Gottwein, unpublished
	2	66, 69	BC-1 genomic DNA	
	3	68, 70	BC-1 genomic DNA	
	1+2	EHG4087, 69	PCR 1 and 2	
	Final	EHG4087, 70	PCR 1+2 and 3	
BAX g2	Anneal	97, 98		
BAX g3	Anneal	99, 100		
BAK1 g1	Anneal	5, 6		
BAK1 g2	Anneal	103F, 103R		
BCL2 g1	Anneal	197, 198		
BCL2 g2	Anneal	199, 200		
BCL-W g1	Anneal	219, 220		
BCL-W g2	Anneal	221, 222		

589

590

591 **REFERENCES**

592 1. Cesarman E. 2014. Gammaherpesviruses and lymphoproliferative disorders. Annu Rev
593 Pathol 9:349-72.
594 2. Nador RG, Cesarman E, Chadburn A, Dawson DB, Ansari MQ, Sald J, Knowles DM.
595 1996. Primary effusion lymphoma: a distinct clinicopathologic entity associated with the
596 Kaposi's sarcoma-associated herpes virus. Blood 88:645-56.
597 3. Lurain K, Polizzotto MN, Aleman K, Bhutani M, Wyvill KM, Goncalves PH, Ramaswami
598 R, Marshall VA, Miley W, Steinberg SM, Little RF, Wilson W, Filie AC, Pittaluga S, Jaffe
599 ES, Whitby D, Yarchoan R, Uldrick TS. 2019. Viral, immunologic, and clinical features of
600 primary effusion lymphoma. Blood 133:1753-1761.
601 4. Jenner RG, Maillard K, Cattini N, Weiss RA, Boshoff C, Wooster R, Kellam P. 2003.
602 Kaposi's sarcoma-associated herpesvirus-infected primary effusion lymphoma has a
603 plasma cell gene expression profile. Proc Natl Acad Sci U S A 100:10399-404.
604 5. Klein U, Gloghini A, Gaidano G, Chadburn A, Cesarman E, Dalla-Favera R, Carbone A.
605 2003. Gene expression profile analysis of AIDS-related primary effusion lymphoma
606 (PEL) suggests a plasmablastic derivation and identifies PEL-specific transcripts. Blood
607 101:4115-21.
608 6. Fan W, Bubman D, Chadburn A, Harrington WJ, Jr., Cesarman E, Knowles DM. 2005.
609 Distinct subsets of primary effusion lymphoma can be identified based on their cellular
610 gene expression profile and viral association. J Virol 79:1244-51.
611 7. Carbone A, Gloghini A, Cozzi MR, Capello D, Steffan A, Monini P, De Marco L, Gaidano
612 G. 2000. Expression of MUM1/IRF4 selectively clusters with primary effusion lymphoma
613 among lymphomatous effusions: implications for disease histogenesis and
614 pathogenesis. Br J Haematol 111:247-57.
615 8. Petre CE, Sin SH, Dittmer DP. 2007. Functional p53 signaling in Kaposi's sarcoma-
616 associated herpesvirus lymphomas: implications for therapy. J Virol 81:1912-22.
617 9. Bubman D, Guasparri I, Cesarman E. 2007. Deregulation of c-Myc in primary effusion
618 lymphoma by Kaposi's sarcoma herpesvirus latency-associated nuclear antigen.
619 Oncogene 26:4979-86.
620 10. Gaidano G, Capello D, Cilia AM, Gloghini A, Perin T, Quattrone S, Migliazza A, Lo Coco
621 F, Saglio G, Ascoli V, Carbone A. 1999. Genetic characterization of HHV-8/KSHV-
622 positive primary effusion lymphoma reveals frequent mutations of BCL6: implications for
623 disease pathogenesis and histogenesis. Genes Chromosomes Cancer 24:16-23.
624 11. Roy D, Sin SH, Damania B, Dittmer DP. 2011. Tumor suppressor genes FHIT and
625 WWOX are deleted in primary effusion lymphoma (PEL) cell lines. Blood 118:e32-9.
626 12. Godfrey A, Anderson J, Papanastasiou A, Takeuchi Y, Boshoff C. 2005. Inhibiting
627 primary effusion lymphoma by lentiviral vectors encoding short hairpin RNA. Blood
628 105:2510-8.
629 13. Wies E, Mori Y, Hahn A, Kremmer E, Sturzl M, Fleckenstein B, Neipel F. 2008. The viral
630 interferon-regulatory factor-3 is required for the survival of KSHV-infected primary
631 effusion lymphoma cells. Blood 111:320-7.
632 14. Xiang Q, Ju H, Nicholas J. 2020. USP7-Dependent Regulation of TRAF Activation and
633 Signaling by a Viral Interferon Regulatory Factor Homologue. J Virol 94.
634 15. Xiang Q, Ju H, Li Q, Mei SC, Chen D, Choi YB, Nicholas J. 2018. Human Herpesvirus 8
635 Interferon Regulatory Factors 1 and 3 Mediate Replication and Latency Activities via
636 Interactions with USP7 Deubiquitinase. J Virol 92.
637 16. Chen D, Sandford G, Nicholas J. 2009. Intracellular signaling mechanisms and activities
638 of human herpesvirus 8 interleukin-6. J Virol 83:722-33.

639 17. Bhatt AP, Bhende PM, Sin SH, Roy D, Dittmer DP, Damania B. 2010. Dual inhibition of
640 PI3K and mTOR inhibits autocrine and paracrine proliferative loops in PI3K/Akt/mTOR-
641 addicted lymphomas. Blood 115:4455-63.
642 18. Cousins E, Nicholas J. 2013. Role of human herpesvirus 8 interleukin-6-activated gp130
643 signal transducer in primary effusion lymphoma cell growth and viability. J Virol
644 87:10816-27.
645 19. de Oliveira DE, Ballon G, Cesarman E. 2010. NF-kappaB signaling modulation by EBV
646 and KSHV. Trends Microbiol 18:248-57.
647 20. Gopalakrishnan R, Matta H, Tolani B, Triche T, Jr., Chaudhary PM. 2016.
648 Immunomodulatory drugs target IKZF1-IRF4-MYC axis in primary effusion lymphoma in
649 a cereblon-dependent manner and display synergistic cytotoxicity with BRD4 inhibitors.
650 Oncogene 35:1797-810.
651 21. Manzano M, Gunther T, Ju H, Nicholas J, Bartom ET, Grundhoff A, Gottwein E. 2020.
652 Kaposi's Sarcoma-Associated Herpesvirus Drives a Super-Enhancer-Mediated Survival
653 Gene Expression Program in Primary Effusion Lymphoma. mBio 11.
654 22. Patil A, Manzano M, Gottwein E. 2018. CK1alpha and IRF4 are essential and
655 independent effectors of immunomodulatory drugs in primary effusion lymphoma. Blood
656 132:577-586.
657 23. Sarek G, Kurki S, Enback J, Iotzova G, Haas J, Laakkonen P, Laiho M, Ojala PM. 2007.
658 Reactivation of the p53 pathway as a treatment modality for KSHV-induced lymphomas.
659 J Clin Invest 117:1019-28.
660 24. Sin SH, Roy D, Wang L, Staudt MR, Fakhari FD, Patel DD, Henry D, Harrington WJ, Jr.,
661 Damania BA, Dittmer DP. 2007. Rapamycin is efficacious against primary effusion
662 lymphoma (PEL) cell lines in vivo by inhibiting autocrine signaling. Blood 109:2165-73.
663 25. Keller SA, Schattner EJ, Cesarman E. 2000. Inhibition of NF-kappa B induces apoptosis
664 of KSHV-infected primary effusion lymphoma cells. Blood 96:2537-2542.
665 26. Manzano M, Patil A, Waldrop A, Dave SS, Behdad A, Gottwein E. 2018. Gene
666 essentiality landscape and druggable oncogenic dependencies in herpesviral primary
667 effusion lymphoma. Nat Commun 9:3263.
668 27. Westphal D, Kluck RM, Dewson G. 2014. Building blocks of the apoptotic pore: how Bax
669 and Bak are activated and oligomerize during apoptosis. Cell Death Differ 21:196-205.
670 28. Escudero S, Zaganjor E, Lee S, Mill CP, Morgan AM, Crawford EB, Chen JH, Wales TE,
671 Mourtada R, Luccarelli J, Bird GH, Steidl U, Engen JR, Haigis MC, Opferman JT,
672 Walensky LD. 2018. Dynamic Regulation of Long-Chain Fatty Acid Oxidation by a
673 Noncanonical Interaction between the MCL-1 BH3 Helix and VLCAD. Molecular Cell
674 69:729-+.
675 29. Perciavalle RM, Stewart DP, Koss B, Lynch J, Milasta S, Bathina M, Temirov J, Cleland
676 MM, Pelletier S, Schuetz JD, Youle RJ, Green DR, Opferman JT. 2012. Anti-apoptotic
677 MCL-1 localizes to the mitochondrial matrix and couples mitochondrial fusion to
678 respiration. Nat Cell Biol 14:575-83.
679 30. Germain M, Nguyen AP, Le Grand JN, Arbour N, Vanderluit JL, Park DS, Opferman JT,
680 Slack RS. 2011. MCL-1 is a stress sensor that regulates autophagy in a developmentally
681 regulated manner. Embo Journal 30:395-407.
682 31. Quentmeier H, Geffers R, Hauer V, Nagel S, Pommerenke C, Uphoff CC, Zaborski M,
683 Drexler HG. 2022. Inhibition of MCL1 induces apoptosis in anaplastic large cell
684 lymphoma and in primary effusion lymphoma. Sci Rep 12:1085.
685 32. Kotschy A, Szlavik Z, Murray J, Davidson J, Maragno AL, Le Toumelin-Braizat G,
686 Chanrion M, Kelly GL, Gong JN, Moujalled DM, Bruno A, Csekei M, Paczal A, Szabo
687 ZB, Sipos S, Radics G, Proszenyak A, Balint B, Ondi L, Blasko G, Robertson A,
688 Surgenor A, Dokurno P, Chen I, Matassova N, Smith J, Pedder C, Graham C, Studeny
689 A, Lysiak-Auvity G, Girard AM, Grave F, Segal D, Riffkin CD, Pomilio G, Galbraith LC,

690 Aubrey BJ, Brennan MS, Herold MJ, Chang C, Guasconi G, Cauquil N, Melchiore F,
691 Guigal-Stephan N, Lockhart B, Colland F, Hickman JA, Roberts AW, Huang DC, Wei
692 AH, et al. 2016. The MCL1 inhibitor S63845 is tolerable and effective in diverse cancer
693 models. Nature 538:477-482.
694 33. Pelossof R, Fairchild L, Huang CH, Widmer C, Sreedharan VT, Sinha N, Lai DY, Guan
695 Y, Premsrirut PK, Tschaharganeh DF, Hoffmann T, Thapar V, Xiang Q, Garippa RJ,
696 Ratsch G, Zuber J, Lowe SW, Leslie CS, Fellmann C. 2017. Prediction of potent
697 shRNAs with a sequential classification algorithm. Nat Biotechnol 35:350-353.
698 34. van der Meer D, Barthorpe S, Yang W, Lightfoot H, Hall C, Gilbert J, Francies HE,
699 Garnett MJ. 2019. Cell Model Passports-a hub for clinical, genetic and functional
700 datasets of preclinical cancer models. Nucleic Acids Res 47:D923-D929.
701 35. Sarid R, Sato T, Bohenzky RA, Russo JJ, Chang Y. 1997. Kaposi's sarcoma-associated
702 herpesvirus encodes a functional bcl-2 homologue. Nat Med 3:293-8.
703 36. Cheng EH, Nicholas J, Bellows DS, Hayward GS, Guo HG, Reitz MS, Hardwick JM.
704 1997. A Bcl-2 homolog encoded by Kaposi sarcoma-associated virus, human
705 herpesvirus 8, inhibits apoptosis but does not heterodimerize with Bax or Bak. Proc Natl
706 Acad Sci U S A 94:690-4.
707 37. Tsherniak A, Vazquez F, Montgomery PG, Weir BA, Kryukov G, Cowley GS, Gill S,
708 Harrington WF, Pantel S, Krill-Burger JM, Meyers RM, Ali L, Goodale A, Lee Y, Jiang G,
709 Hsiao J, Gerath WFJ, Howell S, Merkel E, Ghandi M, Garraway LA, Root DE, Golub TR,
710 Boehm JS, Hahn WC. 2017. Defining a Cancer Dependency Map. Cell 170:564-576
711 e16.
712 38. Vikstrom I, Carotta S, Luthje K, Peperzak V, Jost PJ, Glaser S, Busslinger M, Bouillet P,
713 Strasser A, Nutt SL, Tarlinton DM. 2010. Mcl-1 is essential for germinal center formation
714 and B cell memory. Science 330:1095-9.
715 39. Peperzak V, Vikstrom I, Walker J, Glaser SP, LePage M, Coquery CM, Erickson LD,
716 Fairfax K, Mackay F, Strasser A, Nutt SL, Tarlinton DM. 2013. Mcl-1 is essential for the
717 survival of plasma cells. Nat Immunol 14:290-7.
718 40. Carrington EM, Vikstrom IB, Light A, Sutherland RM, Londrigan SL, Mason KD, Huang
719 DC, Lew AM, Tarlinton DM. 2010. BH3 mimetics antagonizing restricted prosurvival Bcl-
720 2 proteins represent another class of selective immune modulatory drugs. Proc Natl
721 Acad Sci U S A 107:10967-71.
722 41. Robinson MJ, Webster RH, Tarlinton DM. 2020. How intrinsic and extrinsic regulators of
723 plasma cell survival might intersect for durable humoral immunity. Immunol Rev 296:87-
724 103.
725 42. Wang C, Zhang L, Ke L, Ding W, Jiang S, Li D, Narita Y, Hou I, Liang J, Li S, Xiao H,
726 Gottwein E, Kaye KM, Teng M, Zhao B. 2020. Primary effusion lymphoma enhancer
727 connectome links super-enhancers to dependency factors. Nat Commun 11:6318.
728 43. Park A, Oh S, Jung KL, Choi UY, Lee HR, Rosenfeld MG, Jung JU. 2020. Global
729 epigenomic analysis of KSHV-infected primary effusion lymphoma identifies functional
730 MYC superenhancers and enhancer RNAs. Proc Natl Acad Sci U S A 117:21618-21627.
731 44. Lam WY, Bhattacharya D. 2018. Metabolic Links between Plasma Cell Survival,
732 Secretion, and Stress. Trends Immunol 39:19-27.
733 45. Wiest DL, Burkhardt JK, Hester S, Hortsch M, Meyer DI, Argon Y. 1990. Membrane
734 biogenesis during B cell differentiation: most endoplasmic reticulum proteins are
735 expressed coordinately. J Cell Biol 110:1501-11.
736 46. Tellier J, Shi W, Minnich M, Liao Y, Crawford S, Smyth GK, Kallies A, Busslinger M, Nutt
737 SL. 2016. Blimp-1 controls plasma cell function through the regulation of immunoglobulin
738 secretion and the unfolded protein response. Nature Immunology 17:323-330.

739 47. McBrayer SK, Cheng JC, Singhal S, Krett NL, Rosen ST, Shanmugam M. 2012. Multiple
740 myeloma exhibits novel dependence on GLUT4, GLUT8, and GLUT11: implications for
741 glucose transporter-directed therapy. Blood 119:4686-97.
742 48. Kuehnle N, Manzano M, Gottwein E. 2022. Cellular FLIP Protects KSHV-Transformed
743 Lymphoma Cells from TRAIL-Independent TRAIL Receptor 1-Mediated Cell Death.
744 bioRxiv doi:https://doi.org/10.1101/2022.08.17.504167.
745 49. De Leo A, Chen HS, Hu CC, Lieberman PM. 2017. Deregulation of KSHV latency
746 conformation by ER-stress and caspase-dependent RAD21-cleavage. PLoS Pathog
747 13:e1006596.
748 50. Johnston BP, Pringle ES, McCormick C. 2019. KSHV activates unfolded protein
749 response sensors but suppresses downstream transcriptional responses to support lytic
750 replication. PLoS Pathog 15:e1008185.
751 51. Kim YJ, Kim Y, Kumar A, Kim CW, Toth Z, Cho NH, Lee HR. 2021. Kaposi's sarcoma-
752 associated herpesvirus latency-associated nuclear antigen dysregulates expression of
753 MCL-1 by targeting FBW7. PLoS Pathog 17:e1009179.
754 52. Wang HW, Trotter MW, Lagos D, Bourboulia D, Henderson S, Makinen T, Elliman S,
755 Flanagan AM, Alitalo K, Boshoff C. 2004. Kaposi sarcoma herpesvirus-induced cellular
756 reprogramming contributes to the lymphatic endothelial gene expression in Kaposi
757 sarcoma. Nat Genet 36:687-93.
758 53. Diepstraten ST, Anderson MA, Czabotar PE, Lessene G, Strasser A, Kelly GL. 2022.
759 The manipulation of apoptosis for cancer therapy using BH3-mimetic drugs. Nat Rev
760 Cancer 22:45-64.
761 54. Roberts AW, Davids MS, Pagel JM, Kahl BS, Puvvada SD, Gerecitano JF, Kipps TJ,
762 Anderson MA, Brown JR, Gressick L, Wong S, Dunbar M, Zhu M, Desai MB, Cerri E,
763 Heitner Enschede S, Humerickhouse RA, Wierda WG, Seymour JF. 2016. Targeting
764 BCL2 with Venetoclax in Relapsed Chronic Lymphocytic Leukemia. N Engl J Med
765 374:311-22.
766 55. Davids MS, Roberts AW, Seymour JF, Pagel JM, Kahl BS, Wierda WG, Puvvada S,
767 Kipps TJ, Anderson MA, Salem AH, Dunbar M, Zhu M, Peale F, Ross JA, Gressick L,
768 Desai M, Kim SY, Verdugo M, Humerickhouse RA, Gordon GB, Gerecitano JF. 2017.
769 Phase I First-in-Human Study of Venetoclax in Patients With Relapsed or Refractory
770 Non-Hodgkin Lymphoma. J Clin Oncol 35:826-833.
771 56. Davids MS, Roberts AW, Kenkre VP, Wierda WG, Kumar A, Kipps TJ, Boyer M, Salem
772 AH, Pesko JC, Arzt JA, Mantas M, Kim SY, Seymour JF. 2021. Long-term Follow-up of
773 Patients with Relapsed or Refractory Non-Hodgkin Lymphoma Treated with Venetoclax
774 in a Phase I, First-in-Human Study. Clin Cancer Res 27:4690-4695.
775 57. Konopleva M, Pollyea DA, Potluri J, Chyla B, Hogdal L, Busman T, McKeegan E, Salem
776 AH, Zhu M, Ricker JL, Blum W, DiNardo CD, Kadia T, Dunbar M, Kirby R, Falotico N,
777 Leverson J, Humerickhouse R, Mabry M, Stone R, Kantarjian H, Letai A. 2016. Efficacy
778 and Biological Correlates of Response in a Phase II Study of Venetoclax Monotherapy in
779 Patients with Acute Myelogenous Leukemia. Cancer Discov 6:1106-1117.
780 58. Castaneda AF, Glaunsinger BA. 2019. The Interaction between ORF18 and ORF30 Is
781 Required for Late Gene Expression in Kaposi's Sarcoma-Associated Herpesvirus. J Virol
782 93.
783 59. Upreti M, Chu R, Galitovskaya E, Smart SK, Chambers TC. 2008. Key role for Bak
784 activation and Bak-Bax interaction in the apoptotic response to vinblastine. Mol Cancer
785 Ther 7:2224-32.
786 60. Seiler CY, Park JG, Sharma A, Hunter P, Surapaneni P, Sedillo C, Field J, Algar R,
787 Price A, Steel J, Throop A, Fiacco M, LaBaer J. 2014. DNASU plasmid and PSI:Biology-
788 Materials repositories: resources to accelerate biological research. Nucleic Acids Res
789 42:D1253-60.

790 61. Doench JG, Fusi N, Sullender M, Hegde M, Vaimberg EW, Donovan KF, Smith I,
791 Tothova Z, Wilen C, Orchard R, Virgin HW, Listgarten J, Root DE. 2016. Optimized
792 sgRNA design to maximize activity and minimize off-target effects of CRISPR-Cas9. Nat
793 Biotechnol 34:184-191.
794 62. Ran FA, Hsu PD, Wright J, Agarwala V, Scott DA, Zhang F. 2013. Genome engineering
795 using the CRISPR-Cas9 system. Nat Protoc 8:2281-2308.
796

797

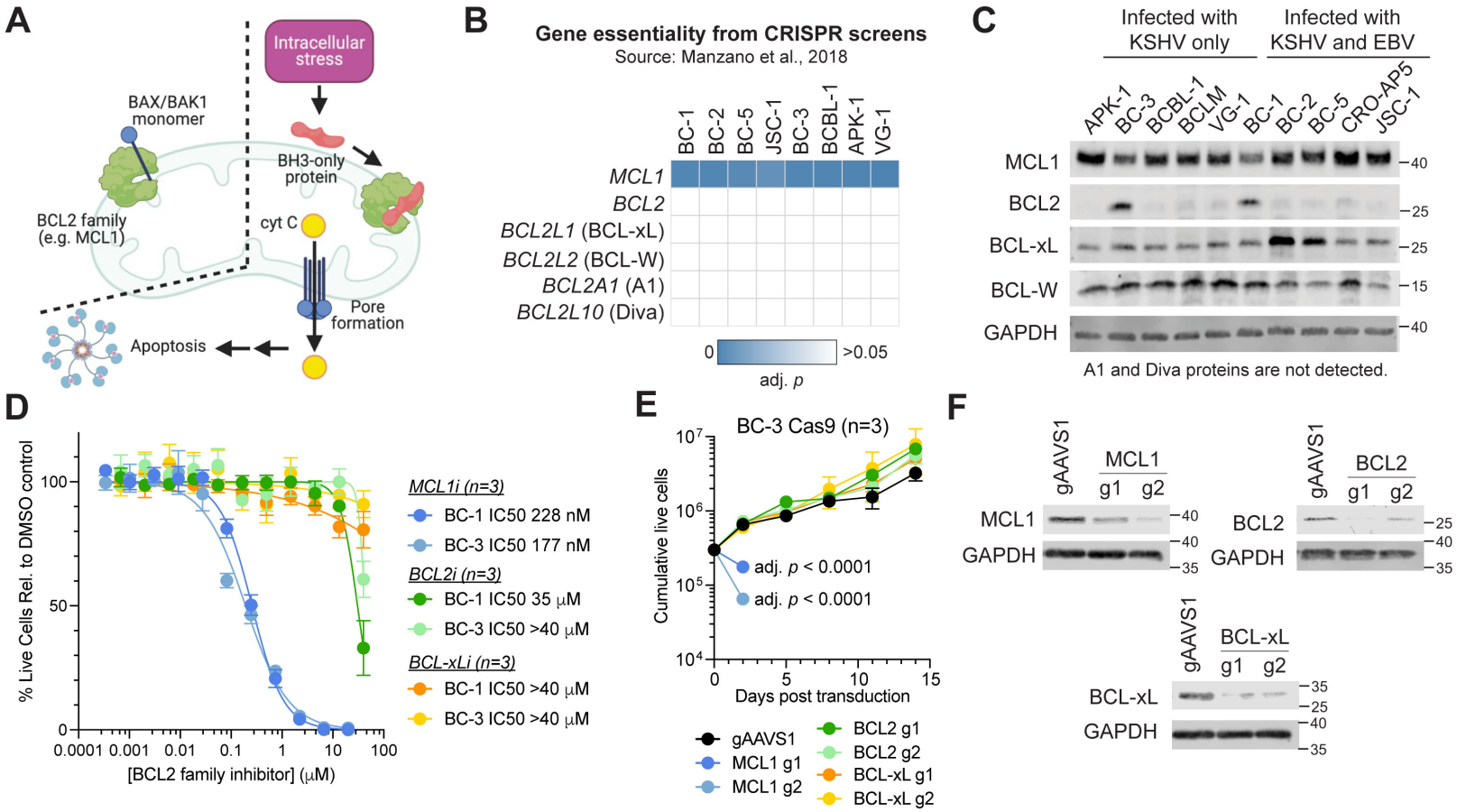
A
Intracellular stress
BAX/BAK1 monomer
BH3-only protein
BCL2 family (e.g. MCL1)
cyt C
Pore formation
Apoptosis
B
Gene essentiality from CRISPR screens
Source: Manzano et al., 2018
BC-1
BC-2
BC-5
JSC-1
BC-3
BCBL-1
APK-1
VG-1
MCL1
BCL2
BCL2L1 (BCL-xL)
BCL2L2 (BCL-W)
BCL2A1 (A1)
BCL2L10 (Diva)
0
>0.05
adj. p
C
Infected with KSHV only
Infected with KSHV and EBV
APK-1
BC-3
BCBL-1
BCLM
VG-1
BC-1
BC-2
BC-5
CRO-AP5
JSC-1
MCL1
BCL2
BCL-xL
BCL-W
GAPDH
40
25
25
15
40
A1 and Diva proteins are not detected.
D
% Live Cells Rel. to DMSO control
100
50
0
0.0001 0.001 0.01 0.1 1 10 100
[BCL2 family inhibitor] (μM)
MCL1i (n=3)
BC-1 IC50 228 nM
BC-3 IC50 177 nM
BCL2i (n=3)
BC-1 IC50 35 μM
BC-3 IC50 >40 μM
BCL-xLi (n=3)
BC-1 IC50 >40 μM
BC-3 IC50 >40 μM
E
BC-3 Cas9 (n=3)
Cumulative live cells
10^7
10^6
10^5
10^4
0 5 10 15
Days post transduction
adj. p < 0.0001
adj. p < 0.0001
gAAVS1
MCL1 g1
MCL1 g2
BCL2 g1
BCL2 g2
BCL-xL g1
BCL-xL g2
F
gAAVS1
MCL1
g1 g2
MCL1
GAPDH
40
40
35
gAAVS1
BCL2
g1 g2
BCL2
GAPDH
25
40
35
gAAVS1
BCL-xL
g1 g2
BCL-xL
GAPDH
35
25
40
35

A

Locus	BC-1 #28 *BAX*$^{-/-}$*BAK1*$^{-/-}$	BC-3 #12 *BAX*$^{-/-}$*BAK1*$^{-/-}$
BAX	Allele 1: Ex3 +1, Δ3, T-G Allele 2: Ex3 Δ115 band	No wt band by PCR Ex3 Δ115 band only
BAK1	Allele 1: Rearranged Ex3-4 Allele 2: Ex3-4 Δ249	No wt band by PCR Ex3 ins115, Ex4 Δ58

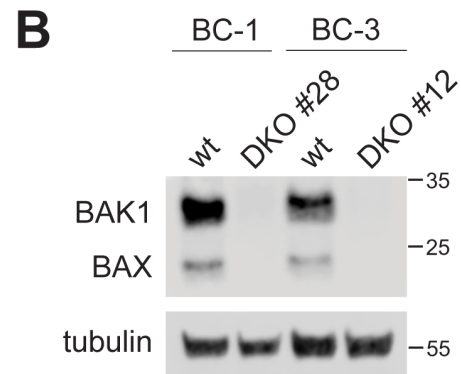

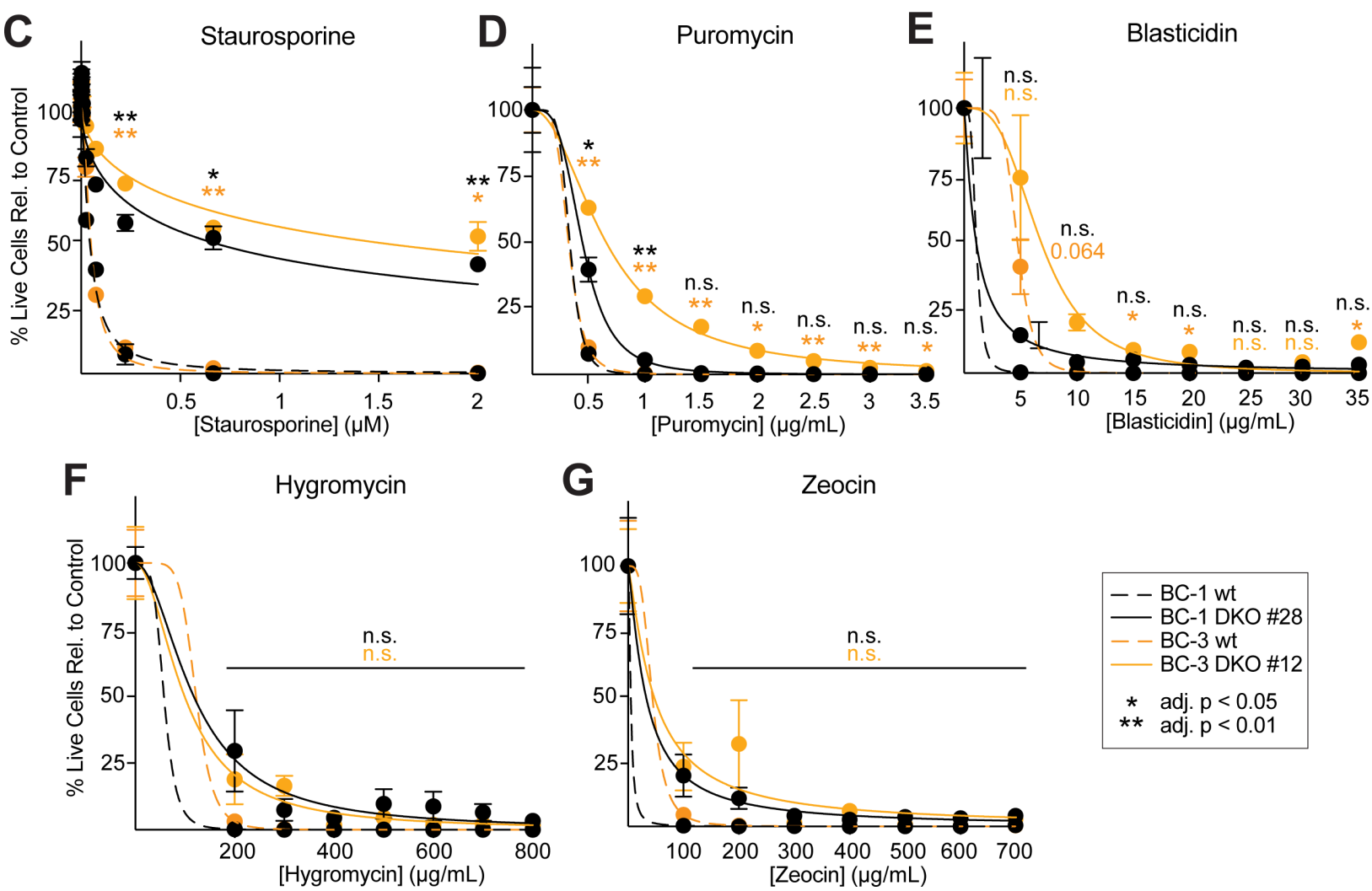

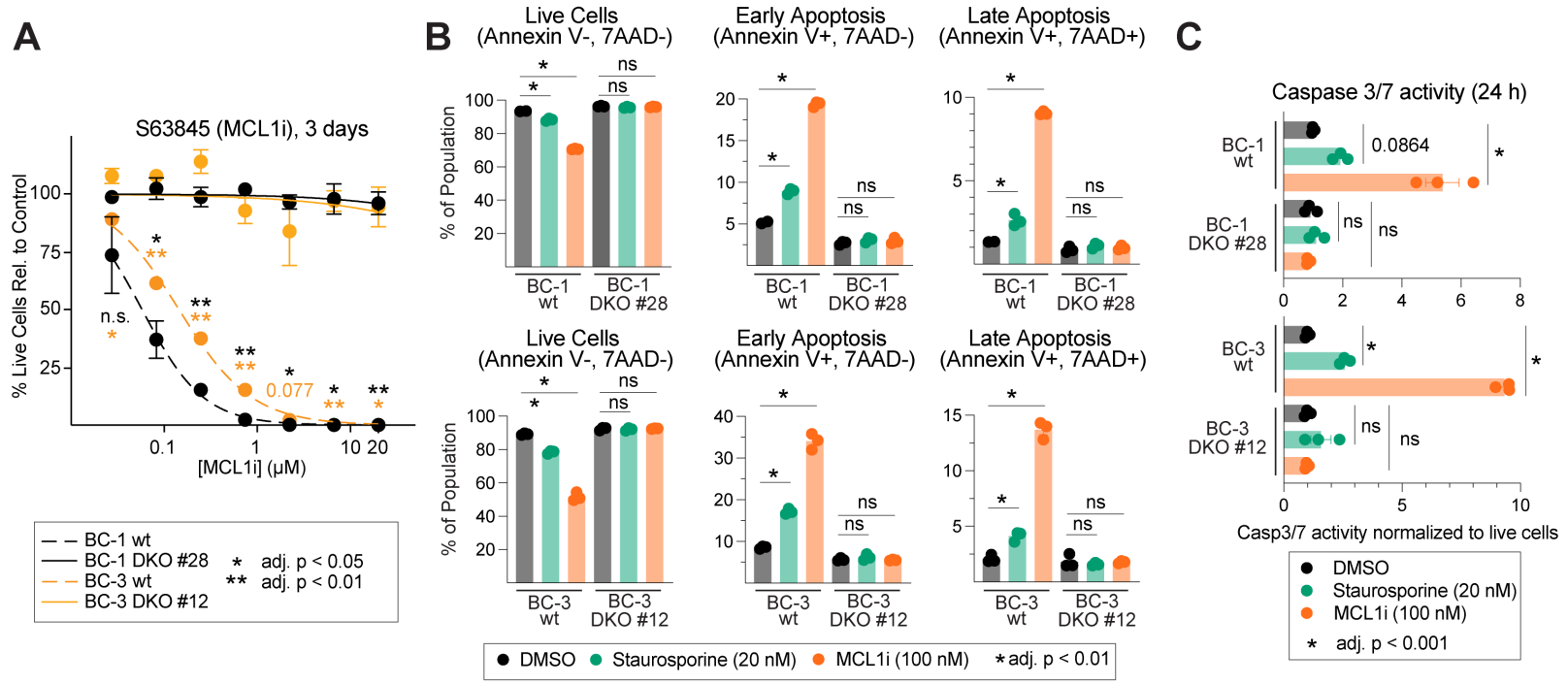
A
S63845 (MCL1i), 3 days
% Live Cells Rel. to Control
[MCL1i] (μM)
n.s.
0.077
BC-1 wt
BC-1 DKO #28
BC-3 wt
BC-3 DKO #12
* adj. p < 0.05
** adj. p < 0.01
B
Live Cells (Annexin V-, 7AAD-)
Early Apoptosis (Annexin V+, 7AAD-)
Late Apoptosis (Annexin V+, 7AAD+)
% of Population
BC-1 wt
BC-1 DKO #28
BC-3 wt
BC-3 DKO #12
ns
DMSO
Staurosporine (20 nM)
MCL1i (100 nM)
* adj. p < 0.01
C
Caspase 3/7 activity (24 h)
0.0864
Casp3/7 activity normalized to live cells
DMSO
Staurosporine (20 nM)
MCL1i (100 nM)
* adj. p < 0.001

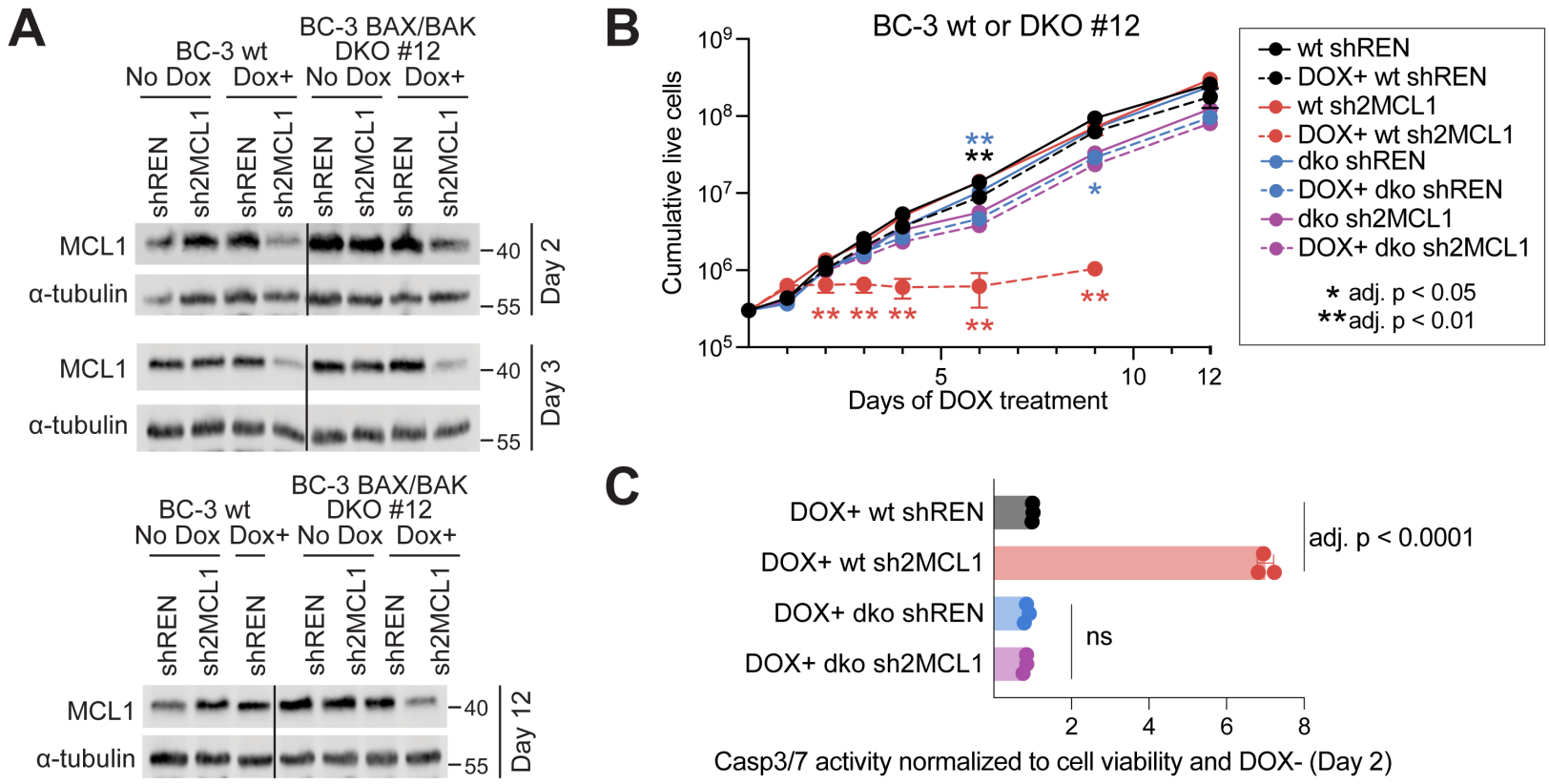
A
BC-3 wt
BC-3 BAX/BAK DKO #12
No Dox
Dox+
No Dox
Dox+
shREN
sh2MCL1
shREN
sh2MCL1
shREN
sh2MCL1
shREN
sh2MCL1
MCL1
α-tubulin
40
55
Day 2
Day 3
Day 12
B
BC-3 wt or DKO #12
Cumulative live cells
Days of DOX treatment
wt shREN
DOX+ wt shREN
wt sh2MCL1
DOX+ wt sh2MCL1
dko shREN
DOX+ dko shREN
dko sh2MCL1
DOX+ dko sh2MCL1
* adj. p < 0.05
** adj. p < 0.01
C
DOX+ wt shREN
DOX+ wt sh2MCL1
DOX+ dko shREN
DOX+ dko sh2MCL1
adj. p < 0.0001
ns
Casp3/7 activity normalized to cell viability and DOX- (Day 2)

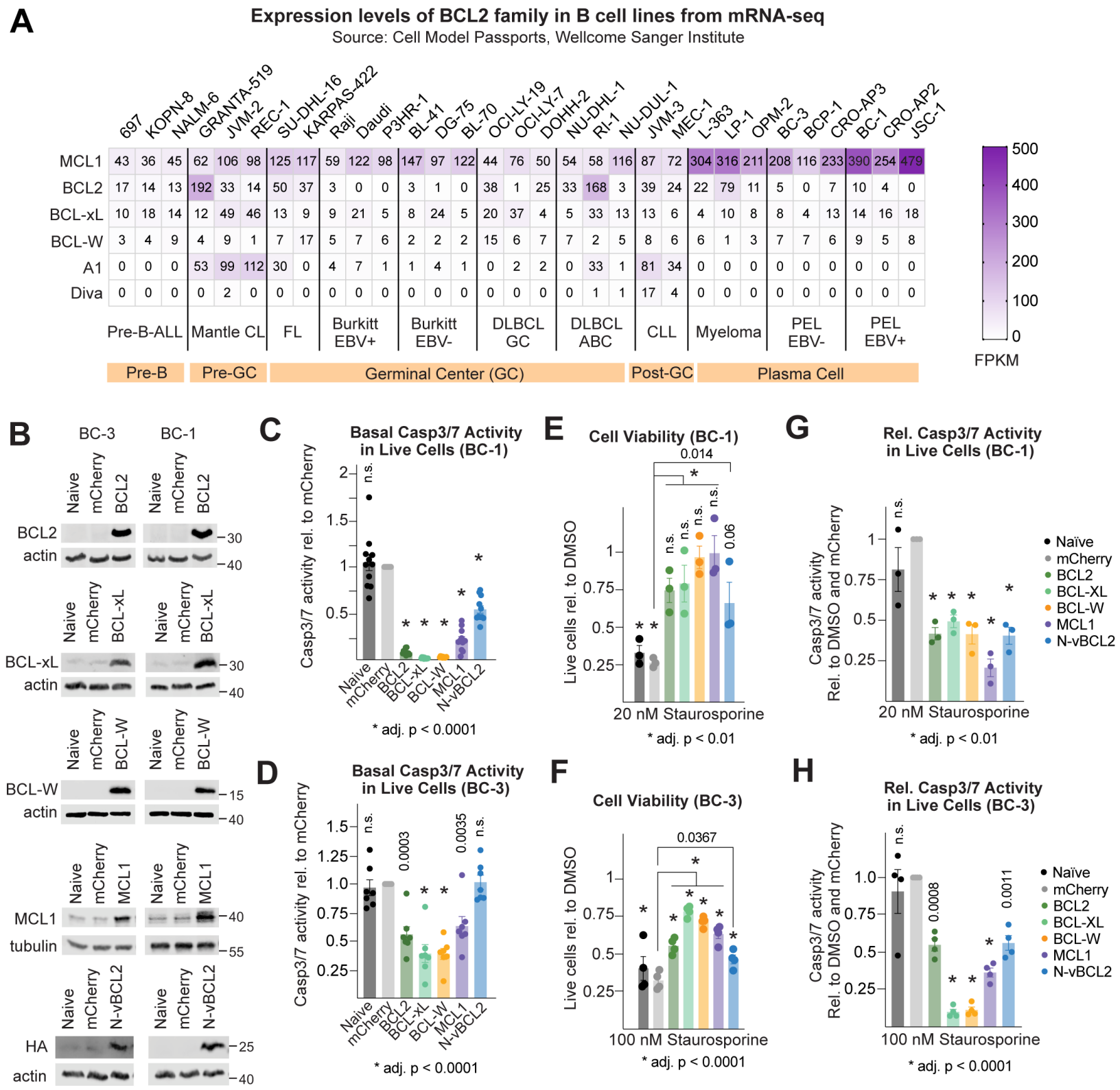
A
Expression levels of BCL2 family in B cell lines from mRNA-seq
Source: Cell Model Passports, Wellcome Sanger Institute
697 KOPN-8 NALM-6 GRANTA-519 JVM-2 REC-1 SU-DHL-16 KARPAS-422 Raji Daudi P3HR-1 BL-41 DG-75 BL-70 OCI-LY-19 OCI-LY-7 DOHH-2 NU-DHL-1 RI-1 NU-DUL-1 JVM-3 MEC-1 L-363 LP-1 OPM-2 BC-3 BCP-1 CRO-AP3 BC-1 CRO-AP2 JSC-1
MCL1 43 36 45 62 106 98 125 117 59 122 98 147 97 122 44 76 50 54 58 116 87 72 304 316 211 208 116 233 390 254 479
BCL2 17 14 13 192 33 14 50 37 3 0 0 3 1 0 38 1 25 33 168 3 39 24 22 79 11 5 0 7 10 4 0
BCL-xL 10 18 14 12 49 46 13 9 9 21 5 8 24 5 20 37 4 5 33 13 13 6 4 10 8 8 4 13 14 16 18
BCL-W 3 4 9 4 9 1 7 17 5 7 6 2 2 2 15 6 7 7 2 5 8 6 6 1 3 7 7 6 9 5 8
A1 0 0 0 53 99 112 30 0 4 7 1 1 4 1 0 2 2 0 33 1 81 34 0 0 0 0 0 0 0 0 0
Diva 0 0 0 0 2 0 0 0 0 0 0 0 0 0 0 0 0 0 1 1 17 4 0 0 0 0 0 0 0 0 0
Pre-B-ALL
Mantle CL
FL
Burkitt EBV+
Burkitt EBV-
DLBCL GC
DLBCL ABC
CLL
Myeloma
PEL EBV-
PEL EBV+
Pre-B
Pre-GC
Germinal Center (GC)
Post-GC
Plasma Cell
500
400
300
200
100
0
FPKM
B
BC-3
BC-1
Naive mCherry BCL2
BCL2
actin
30
40
Naive mCherry BCL-xL
BCL-xL
actin
30
40
Naive mCherry BCL-W
BCL-W
actin
15
40
Naive mCherry MCL1
MCL1
tubulin
40
55
Naive mCherry N-vBCL2
HA
actin
25
40
C
Basal Casp3/7 Activity in Live Cells (BC-1)
Casp3/7 activity rel. to mCherry
n.s.
Naive mCherry BCL2 BCL-xL BCL-W MCL1 N-vBCL2
* adj. p < 0.0001
D
Basal Casp3/7 Activity in Live Cells (BC-3)
Casp3/7 activity rel. to mCherry
n.s. 0.0003 0.0035 n.s.
Naive mCherry BCL2 BCL-xL BCL-W MCL1 N-vBCL2
* adj. p < 0.0001
E
Cell Viability (BC-1)
Live cells rel. to DMSO
0.014
n.s. n.s. n.s. 0.06
20 nM Staurosporine
* adj. p < 0.01
F
Cell Viability (BC-3)
Live cells rel. to DMSO
0.0367
100 nM Staurosporine
* adj. p < 0.0001
G
Rel. Casp3/7 Activity in Live Cells (BC-1)
Casp3/7 activity Rel. to DMSO and mCherry
n.s.
20 nM Staurosporine
* adj. p < 0.01
Naïve
mCherry
BCL2
BCL-XL
BCL-W
MCL1
N-vBCL2
H
Rel. Casp3/7 Activity in Live Cells (BC-3)
Casp3/7 activity Rel. to DMSO and mCherry
n.s. 0.0008 0.0011
100 nM Staurosporine
* adj. p < 0.0001
Naïve
mCherry
BCL2
BCL-XL
BCL-W
MCL1
N-vBCL2

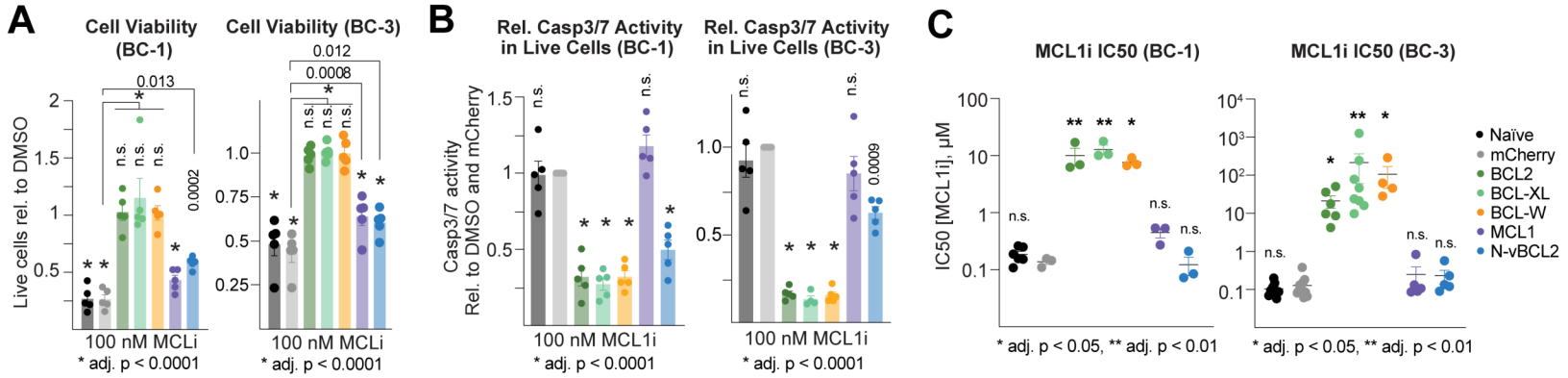
A
Cell Viability (BC-1)
Cell Viability (BC-3)
Live cells rel. to DMSO
0.013
0.0002
0.012
0.0008
n.s.
100 nM MCLi
* adj. p < 0.0001
B
Rel. Casp3/7 Activity in Live Cells (BC-1)
Rel. Casp3/7 Activity in Live Cells (BC-3)
Casp3/7 activity Rel. to DMSO and mCherry
0.0009
100 nM MCL1i
* adj. p < 0.0001
C
MCL1i IC50 (BC-1)
MCL1i IC50 (BC-3)
IC50 [MCL1i], µM
* adj. p < 0.05, ** adj. p < 0.01
Naïve
mCherry
BCL2
BCL-XL
BCL-W
MCL1
N-vBCL2